

THE USE OF NITROGEN AND ETHANE IN  
SURFACE AREA MEASUREMENTS BY ADSORPTION

A THESIS

Presented to  
the Faculty of the Division of Graduate Studies  
Georgia Institute of Technology

In Partial Fulfillment  
of the Requirements for the Degree  
Master of Science in Chemical Engineering

by  
Otto Marucci Morris, Jr.

June 1950

239150

*Crossland*

THE USE OF NITROGEN AND ETHANE IN  
SURFACE AREA MEASUREMENTS BY ADSORPTION

Approved:

*[Signature]*

Date approved by Chairman

*June 30 1950*

## ACKNOWLEDGMENTS

I wish to express my sincere appreciation to Professor J. M. DallaValle for his suggestion of the problem, and for his guidance during its completion. I am also grateful to Mr. Clyde Orr, Jr., of the Micromeritics Laboratory for his valuable aid in the construction of the apparatus and other phases of the work.

## TABLE OF CONTENTS

	PAGE
Approval Sheet . . . . .	ii
Acknowledgments . . . . .	iii
List of Tables . . . . .	v
List of Figures . . . . .	vii
Summary . . . . .	1
Introduction . . . . .	2
Apparatus . . . . .	6
Experimental Procedure . . . . .	8
A. BET Technique . . . . .	8
B. BET(m) Technique . . . . .	10
Discussion of Results . . . . .	16
Nomenclature . . . . .	29
Bibliography . . . . .	31
Appendix I, Derivation of Equations . . . . .	34
Appendix II, Sample Calculations . . . . .	40
Appendix III, Tables . . . . .	44
Appendix IV, Figures . . . . .	70



## LIST OF TABLES

TABLE	PAGE
I. Surface Areas of Samples Tested . . . . .	45
II. Adsorption of Nitrogen by Activated Charcoal. . . . .	46
III. Adsorption of Nitrogen by Activated Charcoal. . . . .	46
IV. Adsorption of Nitrogen by Activated Charcoal. . . . .	47
V. Adsorption of Nitrogen by Activated Charcoal. . . . .	47
VI. Adsorption of Nitrogen by Carbon Black MO-647 . . . . .	48
VII. Adsorption of Nitrogen by Carbon Black MO-647 . . . . .	48
VIII. Adsorption of Nitrogen by Unsized Halloysite. . . . .	49
IX. Adsorption of Nitrogen by Unsized Halloysite. . . . .	49
X. Adsorption of Nitrogen by Unsized Halloysite. . . . .	50
XI. Adsorption of Nitrogen by Kaolinite . . . . .	50
XII. Adsorption of Nitrogen by Kaolinite . . . . .	51
XIII. Adsorption of Nitrogen by Kaolinite . . . . .	51
XIV. Adsorption of Nitrogen by Kaolinite . . . . .	52
XV. Adsorption of Nitrogen by Kaolinite . . . . .	52
XVI. Adsorption of Nitrogen by Kaolinite . . . . .	53
XVII. Adsorption of Nitrogen by Quartz Sand . . . . .	53
XVIII. Adsorption of Nitrogen by Quartz Sand . . . . .	54
XIX. Adsorption of Nitrogen by Nickel . . . . .	54
XX. Adsorption of Nitrogen by Nickel . . . . .	55
XXI. Adsorption of Nitrogen by Aluminum . . . . .	55
XXII. Adsorption of Nitrogen by 15-Micron Monofilament Nylon . .	56
XXIII. Adsorption of Nitrogen by 15-Micron Monofilament Nylon . .	56
XXIV. Adsorption of Nitrogen by Copper . . . . .	57
XXV. Adsorption of Nitrogen by Attapulugus Clay . . . . .	57

TABLE	PAGE
XXVI. Adsorption of Nitrogen by Manganese Dioxide . . . . .	58
XXVII. Adsorption of Nitrogen by Manganese Dioxide . . . . .	58
XXVIII. Adsorption of Nitrogen by Cadmium . . . . .	59
XXIX. Adsorption of Nitrogen by Spheron 6 Carbon Black . . . . .	59
XXX. Adsorption of Nitrogen by Spheron 6 Carbon Black . . . . .	60
XXXI. Adsorption of Nitrogen by Spheron 6 Carbon Black . . . . .	60
XXXII. Adsorption of Nitrogen by Halloysite, -80+100 Mesh . . . . .	61
XXXIII. Adsorption of Nitrogen by Halloysite, -120+140 Mesh . . . . .	61
XXXIV. Adsorption of Nitrogen by Halloysite, -170+200 Mesh . . . . .	62
XXXV. Adsorption of Nitrogen by Halloysite, -250+270 Mesh . . . . .	62
XXXVI. Adsorption of Nitrogen by Halloysite, -270+325 Mesh . . . . .	63
XXXVII. Adsorption of Nitrogen by Halloysite No. 10 . . . . .	63
XXXVIII. Adsorption of Nitrogen by No. 18 Glass Beads . . . . .	64
XXXIX. Adsorption of Nitrogen by Mica 432 . . . . .	64
XL. Adsorption of Ethane by No. 18 Glass Beads . . . . .	65
XLI. Adsorption of Ethane by No. 18 Glass Beads . . . . .	65
XLII. Adsorption of Ethane by Mica 432 . . . . .	66
XLIII. Adsorption of Ethane by Silica 196 . . . . .	66
XLIV. Adsorption of Ethane by Halloysite No. 10 . . . . .	67
XLV. Adsorption of Ethane by Halloysite No. 10 . . . . .	67
XLVI. Adsorption of Ethane by Halloysite No. 10 . . . . .	67
XLVII. Adsorption of Ethane by Nickel . . . . .	68
XLVIII. Adsorption of Ethane by Cadmium . . . . .	68
XLIX. Adsorption of Ethane by Halloysite, -170+200 Mesh . . . . .	69
L. Adsorption of Ethane by Halloysite, -250+270 Mesh . . . . .	69

## LIST OF FIGURES

FIGURE	PAGE
1. Adsorption of Nitrogen by Activated Charcoal . . . . .	71
2. Adsorption of Nitrogen by Cabot Black MO-647 . . . . .	72
3. Adsorption of Nitrogen by Spheron 6 Carbon Black . . . . .	73
4. Adsorption of Nitrogen by Attapulgus Clay . . . . .	74
5. Adsorption of Nitrogen by Manganese Dioxide . . . . .	75
6. Adsorption of Nitrogen by Kaolinite . . . . .	76
7. Adsorption of Nitrogen by Aluminum . . . . .	77
8. Adsorption of Nitrogen by 15-Micron Monofilament Nylon . . . . .	78
9. Adsorption of Nitrogen by Copper . . . . .	79
10. Adsorption of Nitrogen by Quartz Sand . . . . .	80
11. Adsorption of Nitrogen by Unsized Halloysite . . . . .	81
12. Adsorption of Nitrogen by Five Sized Fractions of Halloysite . . . . .	82
13. Graph of BET Equations for Five Sized Fractions of Halloysite . . . . .	83
14. Adsorption of Ethane by Two Sized Fractions of Halloysite . . . . .	84
15. Adsorption of Nitrogen by Halloysite No. 10 . . . . .	85
16. Adsorption of Ethane by Halloysite No. 10 . . . . .	86
17. Adsorption of Nitrogen by Nickel . . . . .	87
18. Adsorption of Ethane by Nickel . . . . .	88
19. Adsorption of Nitrogen by Cadmium . . . . .	89
20. Adsorption of Ethane by Cadmium . . . . .	90
21. Adsorption of Nitrogen by No. 18 Glass Beads . . . . .	91
22. Adsorption of Ethane by No. 18 Glass Beads . . . . .	92
23. Adsorption of Nitrogen by Mica 432 . . . . .	93
24. Adsorption of Ethane by Mica 432 . . . . .	94
25. Adsorption of Ethane by Silica 196 . . . . .	95

THE USE OF NITROGEN AND ETHANE IN  
SURFACE AREA MEASUREMENTS BY ADSORPTION

SUMMARY

The surface areas of a wide variety of substances were determined using either the BET nitrogen adsorption method, the BET(m) ethane adsorption method, or both. Results ranged from a specific surface value of  $871 \text{ m}^2/\text{gm}$  for activated charcoal to  $0.0597 \text{ m}^2/\text{gm}$  for 35-micron diameter glass beads. The surface of these glass beads as calculated from the microscopically measured median diameter was  $0.0599 \text{ m}^2/\text{gm}$ . This close agreement between results determined both microscopically and by use of the BET(m) ethane adsorption method, indicates the accuracy and usefulness of the BET(m) technique.

Results on samples measured by both techniques showed considerable variation in some instances, as did measurements on various samples of the same material which had been treated differently previous to the adsorption. An attempt is made to explain these discrepancies in the light of the effect of evacuation conditions and heat treatment on sintering and agglomeration.



## INTRODUCTION

The use of powdered materials in industry has increased greatly in recent years, and has caused the measurement of surface areas of fine particles to be investigated extensively. The work of several investigators<sup>3, 8, 10, 11, 34</sup> has been directed toward development of simple methods employing the principles of flow through packed beds of material which permit calculation of an "external" surface area. That is, the surface area calculated by these methods is at best the surface which the particles would have if they were enclosed in smooth envelopes past which the permeating fluid flows. However, most finely divided materials of interest in various fields in science and industry are not composed of smooth, regular particles. Many have large "internal" surface areas contributed by irregular indentations or fine microcapillary cracks in the particles themselves which would not be measured by any flow technique.

The development<sup>5, 6, 7, 18, 19</sup> of a gas adsorption method, hereinafter called the BET method, for measuring the "total" surface area of very finely divided materials is the direct result of the importance of this "internal" surface area in many industrial applications, notably the use of catalysts in the synthesis of ammonia. The total surface of materials is significant for many other applica-

tions such as the crushing of solids<sup>28</sup> and any operation involving adsorption.

Several modifications of the BET apparatus are recorded in the literature<sup>4,8,17</sup> which are merely simplifications of the original, the principle being the same in all cases.

If the point on an adsorption isotherm corresponding to a monomolecular layer can be determined, the volume and hence the number of molecules in the monolayer is known. If the number of molecules in the monolayer be multiplied by the average cross-sectional area of an adsorbed molecule, the product will be the absolute surface area of the adsorbent. The principle and limitations of the BET method will be discussed fully elsewhere.

One important disadvantage of the BET method when nitrogen is used as the adsorbate is that the method is not suitable for measuring total sample surfaces of less than 10,000 sq. cm.<sup>17</sup> However, modifications of this method have been used by several groups of investigators<sup>24,28,41</sup> which permit the measurement of samples having a total surface of as low as 100 sq. cm. The modification used in this work will hereinafter be referred to as the BET(m) method.

The essential difference between the use of nitrogen and some other gas such as, say, ethane in the gas adsorp-

tion method is that the magnitude of the pressures measured to obtain the isotherm is of the order of 300 mm. Hg in the case of nitrogen, but only 0.003 mm. Hg in the case of ethane. The reason for this difference is that in order to obtain an isotherm, equilibrium pressures must be measured up to about three tenths the saturation pressure of the adsorbate at the temperature of the sample. Since ethane has a saturation pressure of about 9 microns at the temperature of liquid oxygen ( $-183^{\circ}\text{C}$ ), a McLeod gage may be used to measure the equilibrium pressures. Use of a McLeod gage rather than a mercury manometer permits very much smaller quantities of adsorbed gas to be measured, thus reducing the total surface necessary for the sample.

When the nature of a material is such that a weight of sample of the order of tens of grams or larger would be required for a BET nitrogen measurement of the surface, the method is impractical because of the large sample tubes and long equilibrium times required, and the inherent errors introduced by these factors. The surface of a material such as this may be accurately determined by means of the BET(m) technique provided a balance is available which will give sufficient accuracy on a weight of sample small enough to have a total surface of not more than about 5,000 sq. cm. An ordinary analytical balance is adequate for any sample if both the BET and BET(m) methods are available for use.

Since both methods are in the development stage, the

literature reveals only a limited amount of data regarding the use of the techniques on various adsorbents, and no data on the use of both methods to measure samples of the same adsorbent. It is the purpose of this investigation to determine the suitability of the two methods for measuring the surface areas of many very different adsorbents, and to compare measurements of several adsorbents obtained by using both techniques. The effect of various surface treatments on BET surface measurements will also be studied.



## APPARATUS

This investigation required the construction and use of two main pieces of apparatus.

The BET nitrogen adsorption apparatus shown in figures 26 and 27 was constructed entirely of pyrex glass. All tubing used except that in the adsorption section,  $V_D$ , and the secondary vacuum system which draws the vacuum on the mercury reservoirs, was 10-mm I.D. to facilitate obtaining a high vacuum. Section  $V_D$  was constructed of 4-mm I.D. tubing.

The two McLeod gages each cover ranges from about 0.01 micron to 500 microns to permit detection of stopcock leaks in various sections of the apparatus, and to determine the pressure in the sample tube during evacuation.

All stopcocks in the apparatus are 3-mm oblique bore except one 10-mm straight bore which separates the pump section from the other sections. A special type of high vacuum grease sold under the trade name of "Apiezon N" was used on all stopcocks and on the  $\frac{1}{8}$  10/30 ground glass joint which seals the sample tube to the system.

A glass diffusion pump filled with "Octoil" and backed by a Cenco Megavac mechanical pump provided the high vacuum needed in the system. The diffusion pump was cooled by a small fan which forced air past copper fins on the diffusion tube.

The BET(m) ethane adsorption apparatus shown in Fig.

28 was also constructed entirely of pyrex glass. All tubing used had an I.D. of 4 mm. The only stopcock in the high vacuum side is a mercury-sealed cock at the top of the gas cut-off leg which may be isolated from the system by raising the mercury into the leg.

The barometric leg is for the purpose of sealing off the McLeod gage at high vacuum, and the sample and gas cut-offs serve to isolate parts of the system at the desired low pressures.

The desired high vacuum is obtained with a National Research Corporation water-cooled metal oil diffusion pump backed by a Cenco Megavac mechanical pump.

The mercury used in both the BET and the BET(m) apparatus was wiped with adsorbent paper to remove much of the surface dirt, sprayed through a dilute nitric acid column several times, sprayed once through a column filled with distilled water, and dried overnight in an oven at 110°C.

Additional apparatus used, other than ordinary laboratory equipment, included a glass blowing torch and accessories, a small spark coil leak tester, several 1-liter and 5-liter "Thermos" vacuum flasks, and two 25-liter copper vacuum containers with accessories for transferring liquid oxygen and liquid nitrogen to other vessels.

## EXPERIMENTAL PROCEDURE

A. BET Technique.— The following description of the BET experimental procedure will be clarified by reference to Figure 26 in Appendix IV.

A known weight of sample preferably having a total surface area of between 2 and 100 m<sup>2</sup> is first attached to the system. While the sample is being heated,\* the system is evacuated to remove water and other adsorbed gases from the sample. This treatment does not remove many of the chemisorbed gases, so that if the material is a metal or in any way has properties favorable to chemisorption, special techniques, i.e., heating at high temperatures, reduction, etc., must be used to remove these gases from the sample.

After the sample cools and the pressure, as measured by the left McLeod gage, reaches about  $10^{-5}$  mm. Hg, the sample stopcock is closed and the adsorption system is isolated by closing the appropriate stopcock and raising the mercury in the manometer to the zero level. The sample is then immersed in a liquid nitrogen bath for determining the volume of the adsorption space,  $V_E + V_S$ , with helium gas. At this temperature the adsorption of helium by the sample and glass walls of the container is negligible, and the greater pressure change resulting in the determination in-

---

\*See "Discussion of Results" for effect of evacuation temperature.

creases the accuracy of the volume measurement.

The steps in determining the adsorption space are as follows: with  $V_B$  held at a low value, helium is led into the space,  $V_T$ , from the helium gas cylinder until a pressure of about 350 mm. Hg is obtained. The stopcock connecting  $V_S$  with the other parts of the system is then opened and the pressure read at equilibrium after the manometer has again been adjusted to the zero level.  $V_S$  may then be calculated from the simple material balance:

$$\frac{P_1 V_T}{T_B} = \frac{P_2 V_T}{T_B} + \frac{P_2 V_E}{T_E} + \frac{P_2 V_S}{T_S}$$

The liquid nitrogen bath is removed and the system evacuated. The stopcock that connects the sample space with the rest of the system is closed, and the sample tube is again immersed in the liquid nitrogen bath.

With  $V_B$  adjusted depending on the total surface of the sample ( $V_B$  is large if the sample has a large surface), the adsorbate is led into the space,  $V_T$ , from the gas cylinder to a convenient initial pressure,  $P_1$ , which experience has shown will result in an equilibrium pressure,  $P_2$ , of the desired magnitude. Great care must be taken in the choice of initial pressures so that the range of equilibrium pressures obtained will give sufficient data to establish the lower portion of the isotherm. The stopcock connecting  $V_S$  with  $V_T$  is opened and the equilibrium pressure,  $P_2$ , read.



The equilibration time here varied from a few seconds to about 15 minutes on the samples tested, depending mostly on total surface of the sample.\*

With the stopcock connecting  $V_S$  and  $V_T$  closed, more adsorbate is led into the space,  $V_T$ , and the above procedure repeated. On successive adsorptions the initial pressure in the sample tube,  $P_0$ , is the same as the previous pressure,  $P_2$ , since the stopcock connecting  $V_S$  with  $V_T$  was closed after the equilibrium pressure,  $P_2$ , was measured.

The above procedure is repeated until sufficient points are obtained to plot the adsorption isotherm. The value of  $V_A$  calculated from equation (1), Appendix I, gives the incremental amount of gas at standard conditions adsorbed on each successive addition of adsorbate.

A sample calculation of a typical run is given in Appendix II.

B. BET(m) Technique.— The following description of the BET(m) experimental procedure will be clarified by reference to Fig. 28 in Appendix IV.

A known weight of sample having a total surface of between 100 and 5,000  $\text{cm}^2$  is sealed to the apparatus at  $V_5$ . The entire system is evacuated and degassed by use of an oxygen-gas torch while the sample is heated to about 250°C.

---

\*See "Discussion of Results".

Little is known of the effect of conditions of evacuation on various adsorbates, but heating overnight while evacuating to less than 0.001 micron has been found to give very satisfactory results.

After the sample activation period just described, the sample section is isolated by raising the mercury into the sample cut-off.

The volumes  $V_4$ ,  $V_5$ ,  $V_6$ , and  $V_7$  may be found by a method similar to that used in the original nitrogen method. The mercury level is lowered in the gas cut-off leg and the stopcock is opened slowly to admit helium to  $V_3$ . During this operation it is essential that the pump cut-off be open, since even a few millimeters pressure difference between the two sides of a cut-off leg will cause a small slug of mercury to be forced up into the top horizontal tubes when the cut-off is lowered. The McLeod gage is also sealed off by raising the mercury level to a position a few centimeters above its normal lowered position. This prevents large quantities of gas from entering the gage when gas is first led into the system. Otherwise considerable time would be required to pump the gage down to the desired initial pressure, but with gas led into  $V_2$  only, the relatively small volume may be evacuated in a few seconds to a point which will give the desired initial pressure when the remaining gas is allowed to expand into the gage ( $V_1$ ).

After the helium is admitted and adjusted to the desired initial pressure by the method described above, all cut-offs are set at their normal levels. At this point it is best to allow approximately two minutes for the pressures in  $V_2$  and  $V_1$  to equalize completely. The pressure  $P_1$  in  $V_3$  is then measured with the gage. The sample cut-off is adjusted to its lower level and the helium expands into  $V_4$ ,  $V_5$ ,  $V_6$ , and  $V_7$ . The final pressure  $P_2$  is measured after allowing a short time for equilibration. Since  $V_3 = V_1 + V_2$ , and  $V_1$  was previously determined from the weight of water needed to fill the gage, while  $V_2$  is known from a previous helium calibration (expanding helium from the gage into  $V_2$  at "zero" pressure), the total volume to the left of the sample cut-off point may be calculated from the ideal gas law relation

$$P_1 V_3 = P_2 [V_3 + (V_4 + V_5 + V_6 + V_7)] .$$

The inside diameter of all tubing in the system is known and the lengths of the sections which contain  $V_5$ ,  $V_6$ , and  $V_7$  may be measured. This enables these volumes to be calculated, and  $V_4$  may be obtained by subtraction from the total volume calculated from the helium calibration.

After the final pressure has been measured, all cut-offs are lowered and the entire system is again evacuated to less than 0.001 micron.

Calculations may be simplified by placing the dry

ice bath in its normal position around  $V_7$  during the helium calibration, and measuring the amount of gas which enters  $V_4$ ,  $V_5$ ,  $V_6$ , and  $V_7$  as if it were all at  $T_1$ . This gives a larger volume ( $V_g$ ) than the actual values, but one which is probably more exact than that which would be obtained by correcting the actual value for the temperature of  $V_7$ . The use of  $V_g$  introduces no error in the calculations since the amount of gas in  $V_4$ ,  $V_5$ ,  $V_6$ , and  $V_7$  is all at the same pressure at any given time, so that

$$\frac{PV_4}{T_1} + \frac{PV_5}{T_1} + \frac{PV_6}{T_1} + \frac{PV_7}{T_7} = P\left(\frac{V_4}{T_1} + \frac{V_5}{T_1} + \frac{V_6}{T_1} + \frac{V_7}{T_7}\right) = KP$$

where  $K$  is a constant. The use of  $V_g$  is exact, since

$$\frac{PV_g}{T_1} = \frac{PV_4}{T_1} + \frac{PV_5}{T_1} + \frac{PV_6}{T_1} + \frac{PV_7}{T_7} = KP,$$

by the very nature of the calibration procedure.

The determination of  $V_g$  by the use of helium is quite time-consuming and may be omitted after one or two determinations, since the change in  $V_g$  when a new sample is attached to the system is so small that it has no measurable effect on the position or shape of the isotherm.

If  $V_g$  has been found by the calibration procedure, it is necessary to evacuate the system to about 0.001 micron before continuing with the determination. If  $V_g$  has been estimated and the helium calibration omitted, the remaining procedure is as given below:



With the sample section still isolated, the vapor pressure bulb immersed in liquid oxygen, the pump cut-off lowered, and the gas cut-off lowered, enough ethane is admitted to the system to allow a small amount to condense in the bulb. Pumping is continued until the system pressure approaches the expected value of the saturation pressure (usually about 10 minutes if the gage was open while ethane was being admitted). The pump cut-off is then raised, and gage readings are taken until the system reaches equilibrium (about 15 minutes).

The saturation pressure having been measured, the pump cut-off is lowered, the oxygen bath is removed from the vapor pressure bulb, and ethane is pumped out until the pressure in the system is one which will give a low equilibrium pressure (about 0.3 micron) when the sample cut-off is lowered. Equilibrium usually requires from 20 to 50 minutes depending on the weight of sample and the amount of its internal surface.

When the equilibrium pressure,  $P_2$ , is attained, the sample cut-off is raised, gas and pump cut-offs are lowered, the McLeod gage is isolated, and enough ethane is admitted to give a second equilibrium pressure of the desired magnitude. This procedure is repeated until enough points have been obtained to plot an isotherm.

The derivation of the equation from which the volume

adsorbed ( $V_A$ ) may be calculated is given in Appendix I, and sample calculations appear in Appendix II.

## DISCUSSION OF RESULTS

Because of the large number of variables affecting the BET and the BET(m) gas adsorption techniques, the work done in this investigation is exploratory rather than conclusive. These indeterminate variables permit few quantitative conclusions, but many interesting qualitative explanations of the results are possible and will be presented later in this discussion. The isotherms from the wide variety of materials tested suggest the necessity of a vast amount of experimental work for a thorough understanding of the meaning of the results from even one type of adsorbent, but it is clear that both techniques are so useful when employed with care that they will probably find extensive application in scientific and industrial fields of investigation.

Figures 1 through 25 in Appendix IV are plots of the isotherms obtained from the materials tested. Table I in Appendix III summarizes the specific surface area data obtained and lists permeameter and optical diameter measurement surface areas obtained from other sources.<sup>37,40</sup> Reference to the table and figures mentioned above is made throughout this discussion.

The BET nitrogen method gave excellent reproducibility for materials with large surface areas, i.e., greater than about  $20 \text{ m}^2/\text{gm}$ , such as the activated charcoals, manganese dioxide, and Attapulugus clay. These results are

shown in figures 1 through 5.

Emmett,<sup>17</sup> who is a recognized authority on the gas adsorption technique, claims an absolute accuracy of only 20% on the method for any determination, because a result differing by this amount is found when various gases are used as the adsorbate on the same material. However, when the same gas was used under similar conditions of adsorption, results were reproducible to within about 1% on the large surface samples mentioned.

The accuracy of the method must necessarily depend upon (1) the accuracy with which point "B",<sup>\*</sup> the point at which a monomolecular layer of gas covers the adsorbent surface, may be determined, and (2) the certainty with which the effective cross-sectional area of the adsorbed gas molecule is known. The selection of point "B" is easy and gives excellent reproducibility on isotherms such as those shown in figures 1 through 5, which have long straight line portions, and experimental points which have a very small average deviation from the curve of best fit. On curves such as those shown for sample 4, figure 6, and for copper powder in figure 9, the location of point "B" is uncertain because of the lack of a well-defined straight line portion in the first case, and because of the relatively wide scat-

---

<sup>\*</sup>Appendix I describes the method for locating this point.

tering of the experimental points in the case of the copper powder. This serves to illustrate the fact that great care must be used if important conclusions are to be drawn from experimental surface values obtained by this method. Isotherms must always be carefully analyzed to determine the possible error in the specific surface calculated from selection of point "B". Different investigators might obtain results on the same material which differ by an amount on the order of 100% for the reasons noted.

Different activation conditions seem to have little effect on the location of point "B" in the case of the charcoals and carbon blacks, since all temperatures involved were below 500°C. These materials sinter only at temperatures near 1,000°C,<sup>4</sup> and adsorbed gases seem to be readily removed at the temperatures used. With materials having characteristics such as these one would expect to obtain good reproducibility such as has been observed in this study.

Some general observations concerning conditions of evacuation seem appropriate at this point. All solid materials which have been exposed to the atmosphere have considerable quantities of nitrogen, oxygen, and water vapor adsorbed on their surfaces. These and other adsorbed gases must first be removed if satisfactory adsorption surface measurements are to be made.

If the adsorbed gases are physically adsorbed (Van der Waal adsorption) they may be easily removed by pumping



until a vacuum of the order of 0.01 micron is attained. Heating to slightly elevated temperatures aids in the removal of these gases from the surface. However, if the nature of the adsorbent is such that much chemisorbed gas is present on the surface, as is the case with metals, the adsorbent must be heated to higher temperatures, or other methods<sup>4</sup> must be used to clean the surface.

Considerable care must be taken when heating the adsorbent to drive off adsorbed gases, since the surface of the adsorbent may be altered by the process known as sintering. Sintering usually is evidenced by a growth or agglomeration of particles,<sup>4</sup> but other effects such as plugging of many of the fine capillaries in the material may be the result. Every adsorbent sinters if the temperature is high enough, and consistent results cannot be obtained if sintering occurs, so that best results can only be achieved when the surface of the material to be investigated can be well cleaned by evacuation without injuring the adsorbent surface.

The BET and BET(m) results listed in Table I may be compared with the permeameter surface values in order to predict quite well the extent of the internal, external, and total surface area of the material being investigated.

Many particulate materials such as quartz sand (Figure 10) are dense solids, whereas substances such as activated charcoal are permeated by a labyrinth of exceedingly

fine capillaries. This is well illustrated by comparing permeameter measurements with the gas adsorption results in Table I and figures 1, 7, 9, 10, and 19. Agreement is close for nylon, quartz sand, copper, aluminum, and cadmium, while activated charcoal has a total surface as measured by the BET method of the order of one thousand times the value of the external surface indicated by permeameter results.

Adsorption of nitrogen by several samples of kaolin-ite is shown in Figure 6. Heat treating increased the total adsorptive capacity of the material at pressures above that at which the monomolecular layer formed, but decreased the total surface area by approximately 6%, based on the original surface area. This can possibly be explained as follows: the sintering process tends to seal the very small capillary cracks by fusing the crack walls together, while larger cracks may be pulled farther apart by the surface tension of the fused material. This increases the surface available to multimolecular layer adsorption, for the very small cracks are probably only a few molecules wide, but the total surface area is decreased.

That the effect of the heat treating process was one of sintering rather than of a reaction with the atmosphere is shown by the fact that the results for the sample heated in a helium atmosphere agreed very well with those for the sample heat treated in air.

In order to determine the effect of degree of evacuation on the shape and position of the isotherm, kaolinite was evacuated to only 2 microns after Run 8a without heating. As may be seen in Figure 6, the second isotherm coincided almost exactly with the first, indicating that the surface of this material could probably be easily cleaned by successive adsorption and pumping off of the gas which is to be used in the determination. That this is not a general result will be shown later when the adsorption of ethane on Halloysite No. 10 (Figure 16) is discussed.

Conditions unfavorable to chemisorption are shown by the desorption runs on kaolinite and unsized halloysite in figures 6 and 11, where the desorption and adsorption curves are fairly close. Here the error introduced in the surface value calculated by using the desorption curve to determine point "B" would only be about 20% at most, while the tendency of nickel to chemisorb as shown in Figure 17 would result in an error of over 300% if the surface area were calculated from the desorption curve.

In Figure 12 are shown isotherms obtained on five sized fractions of halloysite. The BET results in Table I show much less variation with mesh size than do the surfaces calculated from permeameter measurements. This is probably due to the fact that halloysite is permeated by microcapillary pores and cracks which are only a few molecules wide but contribute a large internal surface area which is not



measured by the permeameter method. If this be the case, the change in external surface by sizing would have the small effect observed in the BET measurement relative to the flow technique.

Figure 13 illustrates the results obtained when adsorption data are plotted according to the so-called "BET equation". This equation of the isotherm, derived by Brunauer, Emmett, and Teller,<sup>7</sup> is (in one form),

$$\frac{P_2}{\sum \frac{V_A}{W_S} (P_S - P_2)} = \frac{1}{V_M C} + \frac{(C-1)P_2}{V_M P_S C} \dots \dots \dots (5)$$

where C is a constant and the other terms are as defined in the section entitled "Nomenclature" on page 29. This equation is useful once the fact has been established by the determination of isotherms that a material gives an adsorption isotherm of the type defined by Brunauer<sup>4</sup> as type I or type II. For materials such as this, if the left hand term of equation (5) is plotted against  $P_2/P_S$ , a straight line will result up to a relative pressure,  $P_2/P_S$ , of about 0.3, the slope of which is  $(C-1)/V_M C$ . In general, C is very large, and the slope closely approximates  $1/V_M$ . When this method of plotting the experimental data can be utilized it is necessary to determine only a few points to establish the slope of the curve, since the difference in slope obtained by the use of more points is negligible.<sup>17</sup>

It was found that for most of the adsorbents tested in this investigation, the straight line plot did not give satisfactory results, either because the equation plotted a curve with the experimental data obtained or the points were so scattered that surface values differing by 20-30% could be obtained depending on how the line was drawn through the points. Most of the difficulties, however, were due to the curvature. An example may be seen by reference to Run 26, Figure 12.

The adsorption on all BET runs was at the temperature of liquid nitrogen or liquid air since physical adsorption at these temperatures probably takes place as rapidly as the adsorbate can reach the surface. Any slow effects causing longer equilibration times were probably due to chemisorption, chemical reaction, or solution of adsorbate in adsorbent. Equilibrium time in BET nitrogen determinations ranged from a few seconds to 10 or 15 minutes because of these effects, while BET(m) ethane adsorption required from 25 minutes to as long as an hour. The much longer equilibration times observed in BET(m) determinations are undoubtedly due to the slow process of diffusion which is an important factor at the low operating pressures in the BET(m) apparatus.

In general, isotherms determined on various adsorbents (figures 12, 14, 17, 18, 19, 20, 23, 24) by both BET and BET(m) methods yielded somewhat higher surface values in the

case of the BET(m) ethane adsorption. If any differences in surface areas determined by the two methods were due to the difference in area of the two adsorbed molecules it would be expected that the BET(m) method would give a slightly smaller value for the surface since the ethane molecule is larger than the nitrogen molecule and hence would not be able to penetrate as deeply into the fine cracks and pores of the adsorbent.

The closest agreement (approximately 15%) between the two methods was in the measurements on samples of Mica 432 shown in figures 23 and 24. This adsorbent has a relatively small internal surface even though the gas adsorption measurements indicate a total surface of about five times that shown by the permeameter. This difference may be due to the flat, plate-like structure of small mica particles which would tend to pack in layers and make the permeameter result considerably lower than the true external surface value. For the halloysites shown in figures 12 and 14, the BET(m) technique yielded surface values greater than BET values by about 50%, while Halloysite No. 10 gave a BET surface greater than the BET(m) surface by about 5%.

The results noted above are probably due to the different evacuation conditions used on the various runs. Runs 22-26 were all made after the samples had been evacuated for a few hours to a pressure of about 0.01 micron while being

heated at about 200°C. Runs 36 and 37 were made after the halloysite samples had been evacuated 12 and 14 hours, respectively, at 300°C to a pressure lower than 0.001 micron. It would seem that this difference in evacuation time and conditions caused an increase of 38% and 56% respectively, in surface areas of the materials available to adsorb gas. The latter figure is uncertain since point "B" was determined by extrapolation.

Halloysite No. 10, figures 15 and 16, is the floating portion of a quantity of dialyzed halloysite which was separated by a liquid of density 2.62. This is the fraction of the original material which was observed microscopically to have adsorbed dye from solution while the remaining fraction showed no color change.<sup>40</sup> The BET surface on this sample was higher than the smallest mesh fraction on previous halloysite runs, indicating that this fraction was much more active in adsorption than the fraction having the greater density. The BET(m) surface, though reported in Table I to be about 5% lower than the BET result, could easily be a low value as may be seen from the results on three different runs shown in Figure 16. The difference in adsorptive capacity on the three runs may be explained as before on the basis of the activation period. Sample 33a was evacuated for 10 hours, sample 33b for 1 hour to remove the ethane after Run 33a, and sample 33c for 15 hours. All



were evacuated at approximately the same temperature. The breaks in the isotherms were peculiar to this material and may have been caused by the forcing open or unplugging of many fine capillaries at the higher equilibrium pressures. Figures 18, 20, 22, 24, and 25 illustrate the excellent BET(m) isotherms obtained on various materials which have surface areas too low for good results with the BET method. These may be compared with figures 17, 19, 21, and 23.

The halloysites measured on the BET(m) apparatus all gave isotherms which indicated formation of the monomolecular layer at relative pressures above 0.3, whereas all other materials measured using both techniques adsorbed a monolayer at relative pressures near 0.1. The data are not sufficient to determine whether this was because a true equilibrium had not been established on each successive adsorption when it was assumed to be complete, or because the structure of halloysite is such that the larger ethane molecules require higher relative pressures than nitrogen molecules in order to penetrate the fine cracks and capillaries in the material.

A sample of 35-micron glass beads referred in Table I as "No. 18 Glass Beads" was used to check the absolute accuracy of the BET(m) adsorption technique. The median diameter of these beads was determined from a microscopic size distribution. The specific surface was then calculated from this diameter and from the density determined with a

pycnometer. The surface area of the glass beads calculated from these data was  $599 \text{ cm}^2/\text{gm}$ . A sample of the same beads used in a BET(m) determination yielded the isotherm shown in Figure 22, and the surface area as calculated from point "B" shown in the figure was  $597 \text{ cm}^2/\text{gm}$ . The excellent agreement between optical and BET(m) determinations shows the latter technique to be very accurate when used on a material which has an easily cleaned surface such as the glass beads used here and confirms its suitability for determination of average particle size of materials which have no internal surface.

Since the importance of the activation conditions showed such wide variation throughout the study it seems reasonable to conclude that any absolute accuracy on a given material will depend on an intensive study of the material in question in order to obtain the optimum activation conditions. Good relative values of the surface should be obtained with either technique by using similar evacuation and heating conditions, provided the materials to be compared are similar in nature.

From data obtained in this investigation it may be stated that the two techniques cannot be used interchangeably for obtaining relative surface values unless the optimum activation conditions for the materials being studied are known. The results also suggest that the dividing line for the effective use of the two techniques lies in the region of a sample surface of  $5 \text{ m}^2/\text{gm}$ . Samples having a specific

surface smaller than this may be easily measured using the BET(m) technique, and those with higher surfaces lend themselves well to determinations made with the BET apparatus.

## NOMENCLATURE

The following nomenclature applies to the BET nitrogen adsorption technique. Volumes are in cc., pressures in mm. Hg, temperatures in °K, and weights in grams.

$V_B$  = volume of burette space not filled with mercury,

$V_E$  = volume of space between sample stopcock and surface of liquid nitrogen bath,

$V_S$  = volume of sample tube up to surface of liquid nitrogen bath,

$V_D$  = volume of dead space (all other space not included above into which the adsorbate is admitted),

$V_A$  = volume at S.T.P. of gas adsorbed on the sample,

$V_T = V_B + V_D$ ,

$P_0$  = initial pressure in  $V_S$  and  $V_E$ ,

$P_1$  = initial pressure in  $V_B$  and  $V_D$ ,

$P_2$  = final pressure in  $V_B$ ,  $V_D$ ,  $V_S$ , and  $V_E$  (equilibrium pressure),

$P_S$  = saturation pressure of the adsorbate at the temperature of the sample,

$T_B$  = temperature of  $V_B$  and  $V_D$ ,

$T_S$  = temperature of  $V_S$ ,

$T_E$  = average temperature of  $V_E$ ,

$W_S$  = weight of sample.

For the BET(m) ethane adsorption technique, the applicable nomenclature is as follows, where volumes are in cc., pressures in microns, temperatures in °K, and weights in grams:



$V_A$  = volume at S.T.P. of gas adsorbed,

$V_1$  = volume of McLeod gage and capillary,

$V_2$  = volume from McLeod gage to sample cut-off point, with Hg levels at positions indicated by dotted lines in Fig. 28,

$V_3 = V_1 + V_2$ ,

$V_4$  = all volumes from sample cut-off point to sample not included in  $V_5$ ,  $V_6$ , and  $V_7$ ,

$V_5$  = volume of sample tube immersed in sample bath,

$V_6$  = volume from sample bath level to ice line (point where ice has stopped forming on sample tube),

$V_7$  = volume of dry ice trap below liquid level,

$V_8$  = volume of sample cut-off leg which is isolated from sample when cut-off is raised = volume from lower sample cut-off Hg level to sample cut-off point,

$V_9$  = volume of gas at  $T_1$  in  $V_4 + V_5 + V_6 + V_7$ ; measured with  $V_4$ ,  $V_5$ , and  $V_6$  at  $T_1$ , and  $V_7$  at dry ice temperature ( $-80^\circ\text{C}$ ),

$V_{10} = V_9 - V_5 - V_6$ ,

$P_1$  = initial pressure in  $V_3$ ,

$P_2$  = final pressure in  $V_3$ ,  $V_4$ ,  $V_5$ ,  $V_6$ , and  $V_7$ ,

$P_0$  = initial pressure in  $V_4$ ,  $V_5$ ,  $V_6$ , and  $V_7$ ,

$P_S$  = saturation pressure of adsorbate at  $T_5$ ,

$T_1$  = temperature of  $V_3$  and  $V_4$ ,

$T_5$  = temperature of  $V_5$ ,

$T_6$  = temperature of  $V_6$ ,

$T_7$  = temperature of  $V_7$ .

## BIBLIOGRAPHY

1. Anderson, R. B., and Emmett, P. H., J. Am. Chem. Soc., 70, 1135 (1948)
2. Bangham, D. H., and Massallam, S., Proc. Royal Soc. (London), A 165, 552 (1938)
3. Blaine, R. L., ASTM Bulletin, No. 108, p. 17 (1941)
4. Brunauer, S., The Adsorption of Gases and Vapors, Vol. I Princeton University Press, Princeton, N. J. (1945)
5. Brunauer, S., and Emmett, P. H., J. Am. Chem. Soc., 57, 1754 (1935)
6. Brunauer, S., and Emmett, P. H., J. Am. Chem. Soc., 59, 2682 (1937)
7. Brunauer, S., Emmett, P. H., and Teller, E., J. Am. Chem. Soc., 60, 309 (1938)
8. Bugge, P. E., and Kerlogue, R. H., J. Soc. Chem. Ind., 66, 377 (1947)
9. Carman, P. C., J. Soc. Chem. Ind. (Transactions), 57, 225 (1938)
10. Carman, P. C., ibid., 58, 2 (1939)
11. Carman, P. C., Trans. Inst. Chem. Eng. (London), 15, 150 (1937)
12. Davis, R. T., DeWitt, T. W., and Emmett, P. H., J. Phys. and Colloid Chem., 51, 1232 (1947)
13. Davis, R. T., and DeWitt, T. W., J. Am. Chem. Soc., 70, 1135 (1948)
14. Emmett, P. H., Advances in Colloid Science, 1, 1 (1942)
15. Emmett, P. H., Committee on Catalysis, National Research Council, Twelfth Report, Chapter V. John Wiley and Sons, New York (1939)
16. Emmett, P. H., J. Am. Chem. Soc., 68, 1784 (1946)
17. Emmett, P. H., Symposium on New Methods for Particle Size Determination in the Subsieve Range, Am. Soc. Testing Materials (1941)

18. Emmett, P. H., and Brunauer, S., J. Am. Chem. Soc., 59, 1553 (1937)
19. Emmett, P. H., and Brunauer, S., Trans. Electrochem. Soc., 71, 383 (1937)
20. Emmett, P. H., and Cines, M., J. Phys. and Colloid Chem., 51, 1248 (1947)
21. Emmett, P. H., and Cines, M., ibid., 51, 1329 (1947)
22. Emmett, P. H., Brunauer, S., and Love, K., Soil Science, 45, 57 (1938)
23. Emmett, P. H., and DeWitt, T., Ind. Eng. Chem., Anal. Ed., 13, 28 (1941)
24. Gaudin, A. M., and Hukki, R. T., Am. Inst. Mining and Met. Engrs. Tech. Pub. No. 1779 (1944)
25. Green, H. J., J. Franklin Inst., 204, 713 (1927)
26. Harkins, W. D., and Jura, G., J. Am. Chem. Soc., 66, 1362 (1944)
27. Harkins, W. D., and Jura, G., ibid., 66, 1366 (1944)
28. Johnson, J. F., Axelson, J., and Piret, E. L., Chem. Eng. Prog., 45, 708, (1949)
29. Joyner, L. G., and Emmett, P. H., J. Am. Chem. Soc., 70, 2353 (1948)
30. Joyner, L. G., and Emmett, P. H., ibid., 70, 2359 (1948)
31. Jura, G., and Harkins, W. D., ibid., 68, 1941 (1946)
32. Jura, G., and Harkins, W. D., J. Chem. Phys., 11, 430 (1943)
33. Hendrick, F. B., J. Am. Chem. Soc., 62, 2839 (1940)
34. Lea, F. M., and Nurse, R. W., J. Soc. Chem. Ind., 58, 277 (1939)
35. Livingston, H. K., J. Colloid Sci., 4, 447 (1949)
36. Loeb, L. B., The Kinetic Theory of Gases, p. 353, 2nd ed. McGraw-Hill Book Co., New York (1934)

37. Schweyer, H. E., Associate Professor of Chemical Engineering, Univ. of Florida, Gainesville, Fla.; private communication
38. Smith, W. R., Thornhill, F. S., and Bray, R. I., Ind. Eng. Chem., 33, 1303 (1941)
39. Stokinger, H. E., and Laskin, S., Nucleonics, vol. 6, no. 3, 15 (1950)
40. Unpublished data, Micromeritics Laboratory, State Engineering Experiment Station, Georgia Institute of Technology, Atlanta, Ga.
41. Wooten, L. A., and Brown, C., J. Am. Chem. Soc., 65, 113 (1943)
42. DallaValle, J. M., Micromeritics. Pitman Publishing Co., New York (1948)



APPENDIX I

## Derivation of Equations

## APPENDIX I

A. The BET Nitrogen Adsorption Equation.- In determining a typical point on an adsorption isotherm the initial amount of nitrogen is admitted to  $V_T$  at a pressure  $P_1$ . There is an initial amount of gas in  $V_S$  and  $V_E$  at  $P_0$ . After the sample stopcock is opened and the necessary time for equilibrium has elapsed, the pressure in  $V_S$ ,  $V_E$ , and  $V_T$  is  $P_2$ . Since the initial amount of gas present must equal the final amount of gas plus the volume adsorbed, a simple material balance yields

$$\frac{P_1 V_T}{T_B} + \frac{P_0 V_S}{T_S} + \frac{P_0 V_E}{T_E} = \frac{P_2 V_T}{T_B} + \frac{P_2 V_S}{T_S} + \frac{P_2 V_E}{T_E} + \frac{760 V_A}{273}$$

or simplifying,

$$V_A = \frac{273}{760} \left[ \frac{V_T}{T_B} (P_1 - P_2) - \left( \frac{V_S}{T_S} + \frac{V_E}{T_E} \right) (P_2 - P_0) \right] \dots (1)$$

which is the equation used to calculate the incremental amount of nitrogen adsorbed as each successive added volume of nitrogen is allowed to equilibrate.

$P_1$ ,  $P_2$ , and  $P_0$  are measured on the mercury manometer;  $V_D$  (and hence  $V_T$ ) is known from a previous calibration with helium;  $V_S$  is determined by a helium calibration on each run;  $V_E$  is measured by weighing the amount of mercury required to fill it;  $T_B$  is read from a mercury thermometer immersed in the burette water jacket;  $T_S$  is measured with an oxygen vapor

pressure thermometer; and  $T_E$  is estimated from the positions of the ice line and sample bath level.

Volume of gas adsorbed at S.T.P. versus equilibrium pressure data obtained from successive determinations as described in the section entitled "Experimental Procedure" may be used to construct the so-called adsorption isotherm. When the data yield an "S-shaped isotherm", there is good evidence<sup>17</sup> to indicate that the conditions at which a monomolecular layer of gas covers the surface of the adsorbent is the point at which a tangent drawn to the straight-line portion of the isotherm leaves the curve at the low pressure end. Examples of the location of this point, "B", may be seen by reference to figures 1 through 25 in Appendix IV.

After point "B" is determined, the surface of the sample is calculated in the following manner:

Let  $V_M$  = volume at S.T.P. of gas required to form a monomolecular layer on one gram of sample, in cc/gm,

$16.2 \text{ \AA}^2$  = area occupied by one molecule of adsorbed nitrogen,<sup>17</sup>

$S_w$  = surface area of adsorbent in  $\text{cm}^2/\text{gm}$ ;

then,

$$S_w = V_M \times \frac{1 \text{ mole}}{22,400 \text{ cc}} \times \frac{6.02 \times 10^{23} \text{ molecules}}{\text{mole}} \\ \times \frac{16.2 \text{ \AA}^2}{\text{molecule}} \times \frac{10^{-16} \text{ cm}^2}{\text{\AA}^2}$$

$$\text{or } S_w = 4.36 \times V_M \text{ m}^2/\text{gm} \quad . . . . . (2)$$

B. BET(m) Ethane Adsorption Equation.- The amount of gas in any section of the system at a given time is a function of  $PV/T$ . When a charge of ethane is led into  $V_3$ , the amount of ethane in this volume is given by  $P_1V_3/T_1$ . In general, there will have been some gas left in  $(V_9 - V_8)$  at the previous equilibrium pressure,  $P_2$ , which becomes  $P_0$  for this point. This quantity of gas is given by

$$\frac{P_0V_5}{T_5} + \frac{P_0V_6}{T_6} + \frac{P_0V_4}{T_1} + \frac{P_0V_7}{T_7} - \frac{P_0V_8}{T_1}$$

or

$$(P_0) \left( \frac{V_5}{T_5} + \frac{V_6}{T_6} + \frac{V_4}{T_1} + \frac{V_7}{T_7} \right) - \frac{P_0V_8}{T_1}$$

After the sample cut-off is lowered and equilibrium is attained at  $P_2$ , a simple material balance gives (if pressure is expressed in microns)

$$\begin{aligned} \frac{P_1V_3}{T_1} + P_0 \left( \frac{V_5}{T_5} + \frac{V_6}{T_6} + \frac{V_4}{T_1} + \frac{V_7}{T_7} \right) - \frac{P_0V_8}{T_1} \\ = \frac{P_2V_3}{T_1} + P_2 \left( \frac{V_5}{T_5} + \frac{V_6}{T_6} + \frac{V_4}{T_1} + \frac{V_7}{T_7} \right) + \frac{7.60 \times 10^5 V_A}{273} \end{aligned}$$

or

$$V_A = \frac{273}{7.60 \times 10^5} \left[ \frac{V_3}{T_1} (P_1 - P_2) - \left( \frac{V_5}{T_5} + \frac{V_6}{T_6} + \frac{V_{10}}{T_1} \right) (P_2 - P_0) - \frac{P_0V_8}{T_1} \right] \quad \dots (3)$$

$P_1$ ,  $P_2$ , and  $P_0$  are measured;  $V_5$ ,  $V_6$ , and  $V_8$  are found by measuring the length of tubing and calculating the volumes



of the various segments thereof from the known tube diameter;  $V_{10} = V_9 - V_5 - V_6$ , where  $V_9$  is known either from a helium calibration or by estimation as previously described;  $V_3$  is known from previous calibration;  $T_1$  is read with a mercury thermometer;  $T_5$  is taken to be the temperature of pure liquid oxygen at its normal boiling point; and  $T_6$  is an average temperature estimated from the position of the ice line and sample bath level.

After plotting the isotherm, point "B" is determined exactly as in the nitrogen method described previously in this appendix. Using the monomolecular layer volume indicated by point "B", the surface of the sample is calculated in the following manner:

Let  $V_M$  = volume at S.T.P. of gas required to form a monolayer on one gram of sample, in cc/gm,

$22.5 \text{ \AA}^2$  = area occupied by one molecule of adsorbed ethane,<sup>35</sup>

$S_w$  = surface area of adsorbent in  $\text{cm}^2/\text{gm}$ ,

$L$  = length of sample tube immersed in sample bath, in cm,

$\frac{1.76L}{W_S}$  = surface of sample tube per gram of sample,  $\text{cm}^2/\text{gm}$ ,

then

$$S_w = V_M \times \frac{1 \text{ mole}}{22,400 \text{ cc}} \times \frac{6.02 \times 10^{23} \text{ molecules}}{\text{mole}} \times \frac{22.5 \text{ \AA}^2}{\text{molecule}}$$

$$\times \frac{10^{-16} \text{ cm}^2}{\text{\AA}^2} - \frac{1.76L}{W_S}$$

and

$$S_w = 60.5 \times 10^3 \times V_M \text{ cm}^2/\text{gm} - \frac{1.76L}{W_S} \text{ cm}^2/\text{gm} \quad \dots \dots \dots (4)$$

APPENDIX II

## Sample Calculations

## APPENDIX II

The sample calculations shown below will be clarified by reference to Appendix I.

A. BET Method.— The volume of gas at S.T.P. adsorbed on each successive adsorption is given by:

$$V_A = \frac{273}{760} \left[ \frac{V_T}{T_B}(P_1 - P_2) - \left( \frac{V_S}{T_S} + \frac{V_E}{T_E} \right) (P_2 - P_0) \right]$$

The table shown below solves the equation above for  $V_A$  and supplies the calculations needed to plot the isotherm for adsorption of nitrogen on cadmium shown on page 89 from the table of data on page 59.

$$\textcircled{A} = V_T/T_B = 243/300 = 0.8100$$

$$\textcircled{D} = V_E/T_E = 3.5/290 = 0.0121$$

$$\textcircled{C} = V_S/T_S = 52.0/78.2 = 0.6650$$

$$\textcircled{C} + \textcircled{D} = 0.6771$$

Point	$P_1$	$P_2$	$P_0$	$P_1 - P_2$	$\textcircled{A} \times \textcircled{B}$
1	9.8	4.7	0.0	5.1	3.18
2	14.2	9.7	4.7	4.5	3.65
3	20.5	15.5	9.7	5.0	4.05
4	44.5	31.0	15.5	13.5	10.94
5	134.3	85.4	31.0	48.9	39.61

Point	$P_2 - P_0$	$\textcircled{E} \times \textcircled{C+D}$	$\textcircled{AB} - \textcircled{F}$	$\frac{V_A}{W_S}$	$\sum \frac{V_A}{W_S}$
1	4.7	3.18	0.95	0.34	0.34
2	5.0	3.38	0.27	0.10	0.44
3	5.8	3.93	0.12	0.04	0.48
4	15.5	10.49	0.45	0.16	0.64
5	54.4	36.83	2.78	1.00	1.64

$\sum V_A/W_S$  was plotted vs.  $P_2$  to give the isotherm shown on page 89, point "B" was chosen according to the method described in Appendix I to



be 0.0295 cc/gm. This corresponds to  $V_M$ , equation (2), Appendix I, and

$$S_W = 4.36 \times 0.0295 = 0.13 \text{ m}^2/\text{gm}.$$

B. BET(m) Method.— The volume of gas at S.T.P. adsorbed on each successive adsorption is given by:

$$10^3 \times V_A = \frac{273}{760} \left[ \frac{V_3}{T_1} (P_1 - P_2) - \left( \frac{V_5}{T_5} + \frac{V_6}{T_6} + \frac{V_7}{T_7} + \frac{V_4}{T_1} \right) (P_2 - P_0) - \frac{V_8}{T_1} P_0 \right]$$

The table below solves the equation above for  $V_A \times 10^3$  and supplies the calculations needed to plot the isotherm for adsorption of ethane on cadmium shown on page 90 from the table of data on page 68.

$$\begin{aligned} \textcircled{1} &= V_3/T_1 = 389.8/301.5 = 1.293 & \textcircled{4} &= V_{10}/T_1 = 18.8/301.5 = 0.0624 \\ \textcircled{2} &= V_5/T_5 = 0.2/90 = 0.0022 & \textcircled{5} &= \textcircled{2} + \textcircled{3} + \textcircled{4} = 0.0702 \\ \textcircled{3} &= V_6/T_6 = 1.0/180 = 0.0056 & \textcircled{6} &= V_8/T_1 = 0.8/301.5 = 0.0026 \end{aligned}$$

Point:	$L_1$	$L_2$	$L_0$	$P_1$	$P_2$	$P_0$	$P_1 - P_2$	$\textcircled{1} \times \textcircled{7}$	$P_2 - P_0$
1	97.7	10.1	0.0	8.829	0.094	0.000	8.735	11.29	0.094
2	109.8	17.1	10.1	11.152	0.270	0.094	10.882	14.07	0.176
3	120.4	26.3	17.1	13.409	0.640	0.270	12.769	16.51	0.370
4	121.7	48.7	26.3	13.700	2.194	0.640	11.506	14.88	1.554
5	110.5	61.9	48.7	11.294	3.545	2.194	7.749	10.02	1.351

Point	$\textcircled{5} \times \textcircled{9}$	$\textcircled{6} \times P_0$	$\textcircled{8} - \textcircled{10} - \textcircled{11}$	$10^3 \times V_A$	$10^3 \times V_A/W_S$	$10^3 \times \Sigma V_A/W_S$	$P_2/P_S$
1	0.01	0.00	11.28	4.052	22.95	22.95	0.440
2	0.01	0.00	14.06	5.050	28.60	51.55	0.574
3	0.03	0.00	16.48	5.920	33.52	85.07	0.859
4	0.11	0.00	14.77	5.305	30.04	115.11	2.644
5	0.09	0.01	9.92	3.563	20.18	135.30	4.479

$\Sigma V_A/W_S$  was plotted vs.  $P_2/P_S$  to give the isotherm shown on page

90, point "B" was chosen in the same way as previously described for the nitrogen method to be  $113 \times 10^{-3}$  cc/gm. This corresponds to  $V_M$ , equation (4), Appendix I, and

$$S_W = 60.5 \times 10^3 \times 113 \times 10^{-3} - \frac{1.76}{0.1766} = 6830 \text{ cm}^2/\text{gm}.$$

APPENDIX III

Tables

TABLE I

## Surface Areas of Samples Tested

Figure Number	Table Numbers	Run Numbers	Sample	Surface Area* (m <sup>2</sup> /gm)		
				obtained by		
				Nitrogen	Ethane	Perme-
				BET (m)	BET (m)	Optical
				BET	(c)	(c)
1	II, III, IV, V	1, 2, 3a, 3b	Activated charcoal	871	-	0.741
2	VI, VII	4, 5	Cabot black MO-647	495	-	-
11	VIII, IX, X	6a, 6b, 6c	Unsize halloysite	16.2	-	0.208
6	XI	7	Kaolinite	17.6	-	1.20
6	XII, XIII	8a, 8b	Kaolinite	17.6	-	1.04
6	XIV, XV	9a, 9b	Kaolinite	18.8	-	1.16
6	XVI	10	Kaolinite	17.6	-	-
10	XVII, XVIII	11a, 11b	Quartz sand	0.60a	-	0.25
17, 18	XIX, XX, XLVII	12a, 12b, 34	Nickel	0.19a	0.227	0.17
7	XXI	13	Aluminum	0.27a	-	0.15
8	XXII, XXIII	14, 15	Monofilament nylon	0.16a	-	0.05
9	XXIV	16	Copper	0.30a	-	0.24
4	XXV	17	Attapulugus clay	130.6	-	13.3
5	XXVI, XXVII	18a, 18b	Manganese dioxide	72.3	-	1.38
19, 20	XXVIII, XLVIII	19, 35	Cadmium	0.13a	0.683	0.05
3	XXIX, XXX, XXXI	20, 21a, 21b	Spheron 6 carbon	117	-	-
12, 13	XXXII	22	Halloysite, -80+100	7.98	-	0.086
12, 13	XXXIII	23	Halloysite, -120+140	8.46	-	0.106
12, 13, 14	XXXIV, XLIX	24, 36	Halloysite, -170+200	8.78	12.1	0.124
12, 13, 14	XXXV, L	25, 37	Halloysite, -250+270	8.91	13.9	0.148
12, 13	XXXVI	26	Halloysite, -270+325	10.1	-	0.170
15, 16	XXXVII, XLIV, XLV, XLVI	27, 33a, 33b, 33c	Halloysite No. 10	11.3	10.6	-
21, 22	XXXVIII, XL, XLI	28, 30a, 30b	No. 18 glass beads	0.17a	0.0597	-
23, 24	XXXIX, XLII	29, 31	Mica 432	444	5.09	1.52b
25	XLIII	32b	Silica 196	-	1.14	0.542b
				-	-	0.382b

(a) Indicates order of magnitude only

(b) Reference 37

(c) Reference 40 unless otherwise indicated

\*Surface areas listed are average values where several runs were made



TABLE II

Run 1

Adsorption of Nitrogen by Activated Charcoal

$P_1$	$P_2$	$P_0$	$\sum \frac{V_A}{W_S}$	Constants
28.9	0.8	0.0	5.2	$T_B = 305$ $V_T = 154.1$
87.6	1.2	0.8	21.8	
586.7	11.6	1.2	130.1	$T_S = 88.7$ $V_S = 56.9$
630.6	170.6	11.6	179.9	
613.1	324.2	170.6	198.7	$T_E = 290$ $V_E = 3.5$
632.5	440.9	324.2	208.6	
661.4	521.8	440.9	217.8	$W_S = 0.941$
657.6	574.9	574.9	223.2	

TABLE III

Run 2

Adsorption of Nitrogen by Activated Charcoal

$P_1$	$P_2$	$P_0$	$\sum \frac{V_A}{W_S}$	Constants
204.1	1.2	0.0	76.7	$T_B = 305$ $V_T = 274.1$
213.0	20.3	1.2	144.8	
114.7	51.4	20.3	160.8	$T_S = 88.1$ $V_S = 56.5$
127.6	81.8	51.4	170.1	
168.6	120.6	81.8	178.3	$T_E = 275$ $V_E = 3.5$
329.1	219.3	120.6	194.0	
471.9	346.3	219.3	208.5	$W_S = 0.847$

TABLE IV

Run 3a

Adsorption of Nitrogen by Activated Charcoal

$P_1$	$P_2$	$P_0$	$\sum \frac{V_A}{W_S}$	Constants	
210.2	0.8	0.0	51.2	$T_B = 304$	$V_T = 274.1$
188.3	2.5	0.8	96.5	$T_S = 88.6$	$V_S = 12.4$
211.4	24.5	2.5	141.3	$T_E = 275$	$V_E = 3.5$
106.1	50.8	24.5	153.7	$W_S = 1.325$	
133.2	86.9	50.8	163.5		
180.3	135.1	86.9	172.6		
361.6	270.0	135.1	189.4		
539.0	451.5	270.0	203.0		

TABLE V

Run 3b

Adsorption of Nitrogen by Activated Charcoal

$P_1$	$P_2$	$P_0$	$\sum \frac{V_A}{W_S}$	Constants	
191.9	0.7	0.0	46.7	$T_B = 304$	$V_T = 274.1$
189.6	2.3	0.7	92.5	$T_S = 89.0$	$V_S = 12.4$
197.0	15.8	2.3	136.2	$T_E = 275$	$V_E = 3.5$
98.5	38.6	15.8	150.0	$W_S = 1.325$	
124.2	73.3	38.6	161.0		
159.0	115.0	73.3	160.0		
413.5	292.0	115.0	192.5		
491.6	426.2	292.0	203.0		
630.4	571.7	426.2	211.4		

TABLE VI

Run 4

Adsorption of Nitrogen by Carbon Black MO-647

$P_1$	$P_2$	$P_0$	$\sum \frac{V_A}{W_S}$	Constants	
97.3	22.9	0.0	103.0	$T_B = 300.5^*$ 298.0**	$V_T = 243$
105.7	63.2	22.9	117.5		
118.0	90.3	63.2	125.6	$T_S = 79.5$	$V_S = 54.6$
170.8	130.8	90.3	135.1		
225.1	178.4	130.8	145.6	$T_E = 290$	$V_E = 3.5$
51.3	4.0	0.0	83.4		
56.0	26.1	4.0	104.2	$W_S = 0.154$	
56.3	40.8	26.1	109.6		

\*Applicable to the first five points

\*\*Applicable to the last three points

TABLE VII

Run 5

Adsorption of Nitrogen by Carbon Black MO-647

$P_1$	$P_2$	$P_0$	$\sum \frac{V_A}{W_S}$	Constants	
15.6	0.3	0.0	47.9	$T_B = 301$	$V_T = 243$
18.1	4.1	0.3	82.2		
28.2	14.9	4.1	95.2	$T_S = 79.1$	$V_S = 53.5$
31.7	23.1	14.9	100.3		
51.7	37.7	23.1	105.3	$T_E = 280$	$V_E = 3.5$
75.3	56.7	37.7	113.0		
103.0	79.2	56.7	119.1	$W_S = 0.091$	
124.0	102.3	79.2	125.5		
164.0	134.0	102.3	134.9		
204.1	170.1	134.0	145.2		
247.7	210.2	170.1	155.7		

TABLE VIII

Run 6a

Adsorption of Nitrogen by Unsized Halloysite

$P_1$	$P_2$	$P_0$	$\sum \frac{V_A}{W_S}$	Constants
56.4	17.9	0.0	1.87	$T_B = 303$ $V_T = 273.1$
65.1	41.4	17.9	2.44	
81.5	62.3	41.4	2.81	$T_S = 88.0$ $V_S = 52.7$
86.3	75.6	62.3	2.94	
109.7	94.7	75.6	3.11	$T_E = 290$ $V_E = 3.5$
197.2	153.2	94.7	3.48	
412.8	303.2	153.2	4.18	$W_S = 4.593$
485.9	408.8	303.2	4.66	
626.6	534.8	408.8	5.23	

TABLE IX

Run 6b

Adsorption of Nitrogen by Unsized Halloysite

$P_1$	$P_2$	$P_0$	$\sum \frac{V_A}{W_S}$	Constants
245.7	365.7	534.8	4.70	$T_B = 303$ $V_T = 273.1$
119.6	222.7	365.7	4.14	
63.5	130.4	222.7	3.74	$T_S = 89.7$ $V_S = 52.7$
51.2	85.2	130.4	3.46	
				$T_E = 290$ $V_E = 3.5$
				$W_S = 4.593$

TABLE X

Run 6c

Adsorption of Nitrogen by Unsized Halloysite

$P_1$	$P_2$	$P_0$	$\sum \frac{V_A}{W_S}$	Constants	
56.1	13.9	0.0	1.85	$T_B = 302$	$V_T = 229.1$
80.0	43.9	13.9	2.80		
114.0	79.2	42.9	2.96	$T_S = 88.9$	$V_S = 52.7$
128.2	105.2	97.2	3.09		
244.6	178.7	105.2	3.53	$T_E = 290$	$V_E = 3.5$
362.8	276.7	178.7	4.01		
424.6	355.6	276.7	4.38	$W_S = 4.593$	
625.5	499.6	355.6	5.03		

TABLE XI

Run 7

Adsorption of Nitrogen by Kaolinite

$P_1$	$P_2$	$P_0$	$\sum \frac{V_A}{W_S}$	Constants	
30.2	10.2	0.0	2.59	$T_B = 302$	$V_T = 253.0$
50.3	30.0	10.2	3.22		
86.7	58.8	30.0	3.77	$T_S = 77.3$	$V_S = 56.8$
120.8	90.8	58.8	4.08		
161.1	127.0	90.8	4.55	$T_E = 290$	$V_E = 3.5$
310.3	221.1	127.0	5.81		
456.2	340.6	221.1	7.93	$W_S = 1.274$	
629.2	485.6	340.6	11.30		



TABLE XII

Run 8a

Adsorption of Nitrogen by Kaolinite

$P_1$	$P_2$	$P_0$	$\sum \frac{V_A}{W_S}$	Constants	
23.0	5.8	0.0	2.07	$T_B = 303$	$V_T = 243.0$
43.0	21.8	5.8	3.19		
60.1	40.9	21.8	3.73	$T_S = 77.3$	$V_S = 51.9$
101.2	71.2	40.9	4.44		
129.0	100.4	71.2	5.03	$T_E = 290$	$V_E = 3.5$
203.0	152.3	100.4	6.15		
438.3	296.2	152.3	9.52	$W_S = 1.691$	
591.6	443.1	296.2	13.48		

TABLE XIII

Run 8b

Adsorption of Nitrogen by Kaolinite

$P_1$	$P_2$	$P_0$	$\sum \frac{V_A}{W_S}$	Constants	
33.3	10.0	0.0	2.54	$T_B = 302$	$V_T = 243.0$
63.7	36.0	10.0	3.49		
125.5	81.3	36.0	4.49	$T_S = 77.3$	$V_S = 51.9$
161.0	121.8	81.3	5.32		
258.8	190.7	121.8	6.98	$T_E = 290$	$V_E = 3.5$
364.0	278.6	190.7	8.81		
583.1	431.1	278.6	12.66	$W_S = 1.691$	

TABLE XIV

Run 9a

Adsorption of Nitrogen by Kaolinite

$P_1$	$P_2$	$P_0$	$\sum \frac{V_A}{W_S}$	Constants
505.2	535.4	567.7	6.06	$T_B = 303$ $V_T = 229.1$
541.2	492.5	535.4	5.68	
301.2	392.5	492.5	5.49	$T_S = 87.6$ $V_S = 58.3$
120.3	249.6	392.5	5.35	
64.9	152.4	249.6	5.30	$T_E = 290$ $V_E = 3.5$
52.0	100.3	152.4	5.11	
24.9	61.1	100.3	4.97	$W_S = 2.094$
17.0	38.8	61.1	4.73	
0.0	20.6	38.8	4.15	

TABLE XV

Run 9b

Adsorption of Nitrogen by Kaolinite

$P_1$	$P_2$	$P_0$	$\sum \frac{V_A}{W_S}$	Constants
20.8	3.6	0.0	1.81	$T_B = 304$ $V_T = 229.1$
44.9	20.0	3.6	3.10	
81.8	49.2	20.0	3.87	$T_S = 85.7$ $V_S = 58.3$
100.9	74.9	49.2	4.15	
130.6	103.3	74.9	4.30	$T_E = 290$ $V_E = 3.5$
257.2	182.3	103.3	4.58	
424.3	306.7	182.3	5.01	$W_S = 2.094$
640.2	478.0	306.7	5.68	

TABLE XVI

Run 10

Adsorption of Nitrogen by Kaolinite

$P_1$	$P_2$	$P_0$	$\sum \frac{V_A}{W_S}$	Constants
51.4	18.5	0.0	2.10	$T_B = 305$ $V_T = 229.1$
102.3	57.8	18.5	3.29	
153.4	107.0	57.8	3.58	$T_S = 88.3$ $V_S = 58.3$
172.3	140.5	107.0	3.82	
249.6	197.3	140.5	4.01	$T_E = 290$ $V_E = 3.5$
350.7	277.8	197.3	4.11	
				$W_S = 2.094$

TABLE XVII

Run 11a

Adsorption of Nitrogen by Quartz Sand

$P_1$	$P_2$	$P_0$	$\sum \frac{V_A}{W_S}$	Constants
35.5	17.3	0.0	0.16	$T_B = 303.5$ $V_T = 238.0$
49.1	33.5	17.3	0.21	
83.4	58.9	33.5	0.29	$T_S = 78.0$ $V_S = 55.3$
102.3	80.9	58.9	0.37	
133.8	107.7	80.9	0.47	$T_E = 290$ $V_E = 3.5$
211.2	160.2	107.7	0.68	
302.0	231.0	160.2	1.13	$W_S = 3.801$

TABLE XVIII

Run 11b

Adsorption of Nitrogen by Quartz Sand

$P_1$	$P_2$	$P_0$	$\sum \frac{V_A}{W_S}$	Constants	
6.5	2.8	0.0	0.08	$T_B = 304$	$V_T = 238.0$
10.4	6.4	2.8	0.13	$T_S = 77.5$	$V_S = 55.3$
17.0	11.8	6.4	0.15	$T_E = 290$	$V_E = 3.5$
25.9	18.9	11.8	0.18	$W_S = 3.801$	

TABLE XIX

Run 12a

Adsorption of Nitrogen by Nickel

$P_1$	$P_2$	$P_0$	$\sum \frac{V_A}{W_S}$	Constants	
33.9	17.5	0.0	0.042	$T_B = 299.5$	$V_T = 253.0$
57.2	39.0	17.5	0.046	$T_S = 77.3$	$V_S = 54.6$
84.1	63.1	39.0	0.058	$T_E = 290$	$V_E = 3.5$
104.6	85.3	63.1	0.071	$W_S = 11.110$	
134.0	111.1	85.3	0.100		
232.4	176.0	111.1	0.136		
363.2	275.4	176.0	0.227		
504.0	396.6	275.4	0.346		
632.1	520.9	396.6	0.502		

TABLE XX

Run 12b

## Adsorption of Nitrogen by Nickel

$P_1$	$P_2$	$P_0$	$\sum \frac{V_A}{W_S}$	Constants	
445.3	480.5	520.9	0.481	$T_B = 300.5$	$V_T = 253.0$
431.1	454.5	480.5	0.449	$T_S = 77.3$	$V_S = 54.6$
333.6	390.2	454.5	0.400	$T_E = 290$	$V_E = 3.5$
182.2	279.6	390.2	0.317	$W_S = 11.110$	
90.5	178.4	279.6	0.274		
9.3	88.0	178.4	0.229		
0.0	40.6	88.0	0.223		
0.0	19.0	40.6	0.207		
0.0	9.1	19.0	0.197		

TABLE XXI

Run 13

## Adsorption of Nitrogen by Aluminum

$P_1$	$P_2$	$P_0$	$\sum \frac{V_A}{W_S}$	Constants	
31.6	16.5	0.0	0.060	$T_B = 301$	$V_T = 243$
57.6	38.4	16.5	0.075	$T_S = 78$	$V_S = 53.6$
100.3	70.7	38.4	0.193	$T_E = 290$	$V_E = 3.5$
130.0	102.1	70.7	0.243	$W_S = 3.991$	
197.8	125.2	102.1	0.403		
313.1	236.0	152.2	0.732		
518.8	383.1	236.0	1.333		
650.2	521.6	383.1	1.959		



TABLE XXII

Run 14

Adsorption of Nitrogen by 15-micron Monofilament Nylon

$P_1$	$P_2$	$P_0$	$\sum \frac{V_A}{W_S}$	Constants	
8.8	3.7	0.0	0.0047	$T_B = 300.5$	$V_T = 143$
19.1	9.9	3.7	0.037	$T_S = 78.8$	$V_S = 50.33$
27.2	17.2	9.9	0.038	$T_E = 280$	$V_E = 3.5$
47.3	29.6	17.2	0.072	$W_S = 3.800$	
75.2	48.5	29.6	0.111		
109.7	73.3	48.5	0.223		

TABLE XXIII

Run 15

Adsorption of Nitrogen by 15-micron Monofilament Nylon

$P_1$	$P_2$	$P_0$	$\sum \frac{V_A}{W_S}$	Constants	
4.0	0.6	0.0	-0.00289	$T_B = 299$	$V_T = 29.0$
7.0	1.1	0.6	+0.01298	$T_S = 78.0$	$V_S = 48.06$
9.5	2.4	1.1	0.00510	$T_E = 280$	$V_E = 3.5$
13.0	3.2	2.4	0.03265	$W_S = 5.840$	

TABLE XXIV

Run 16

Adsorption of Nitrogen by Copper

$P_1$	$P_2$	$P_0$	$\sum \frac{V_A}{W_S}$	Constants	
13.8	7.0	0.0	0.0328	$T_B = 300$	$V_T = 243$
22.4	14.9	7.0	0.0634	$T_S = 82.4$	$V_S = 52.4$
33.9	25.2	14.9	0.0674		
50.7	39.0	25.2	0.0742	$T_E = 280$	$V_E = 3.5$
83.5	63.3	39.0	0.0729		
103.1	84.8	63.3	0.0859	$W_S = 8.407$	
123.9	106.1	84.8	0.1055		

TABLE XXV

Run 17

Adsorption of Nitrogen by Attapulugus Clay

$P_1$	$P_2$	$P_0$	$\sum \frac{V_A}{W_S}$	Constants	
80.5	0.6	0.0	10.14	$T_B = 300.5$	$V_T = 243$
105.4	9.9	0.6	21.33	$T_S = 78.5$	$V_S = 53.01$
61.7	24.5	9.9	24.50		
61.2	37.3	24.5	26.17	$T_E = 280$	$V_E = 3.5$
71.1	50.1	37.3	27.47		
99.0	70.0	50.1	29.02	$W_S = 2.276$	
130.7	95.3	70.0	30.80		
197.9	139.2	95.3	33.53		
297.5	207.0	139.2	37.73		
340.8	264.1	207.0	41.33		

TABLE XXVI

Run 18a

Adsorption of Nitrogen by Manganese Dioxide

$P_1$	$P_2$	$P_0$	$\sum \frac{V_A}{W_S}$	Constants	
12.6	0.3	0.0	6.45	$T_B = 301$	$V_T = 243$
32.9	10.8	0.3	13.22	$T_S = 78.5$	$V_S = 56.2$
36.4	23.3	10.8	14.22		
47.8	35.3	23.3	15.11	$T_E = 280$	$V_E = 3.5$
101.4	68.1	35.3	17.11		
150.6	109.7	68.1	18.92	$W_S = 0.541$	
204.6	257.5	109.7	21.05		
311.9	235.1	157.5	24.75		

TABLE XXVII

Run 18b

Adsorption of Nitrogen by Manganese Dioxide

$P_1$	$P_2$	$P_0$	$\sum \frac{V_A}{W_S}$	Constants	
18.7	0.8	0.0	9.21	$T_B = 301.5$	$V_T = 243$
19.3	7.7	0.8	12.15	$T_S = 79.2$	$V_S = 56.2$
35.8	21.0	7.7	13.78		
48.7	34.5	21.0	15.00	$T_E = 280$	$V_E = 3.5$
118.8	76.9	34.5	17.38		
207.4	142.6	76.9	21.00	$W_S = 0.541$	
259.9	252.4	142.6	26.62		

TABLE XXVIII

Run 19

Adsorption of Nitrogen by Cadmium

$P_1$	$P_2$	$P_0$	$\sum \frac{V_A}{W_S}$	Constants
9.8	4.7	0.0	0.02	$T_B = 300$ $V_T = 243$
14.2	9.7	4.7	0.03	
20.5	15.5	9.7	0.03	$T_S = 78.2$ $V_S = 52.0$
44.5	31.0	15.5	0.04	
134.3	85.4	31.0	0.11	$T_E = 290$ $V_E = 3.5$
				$W_S = 14.548$

TABLE XXIX

Run 20

Adsorption of Nitrogen by Spheron 6 Carbon Black

$P_1$	$P_2$	$P_0$	$\sum \frac{V_A}{W_S}$	Constants
15.6	1.2	0.0	10.87	$T_B = 299.5$ $V_T = 243$
23.0	8.7	1.2	17.18	
50.6	27.9	8.7	21.98	$T_S = 78.8$ $V_S = 54.9$
73.0	50.0	27.9	24.97	
104.4	77.0	50.0	28.07	$T_E = 290$ $V_E = 3.5$
130.4	104.0	77.0	30.36	
316.2	211.1	104.0	39.69	$W_S = 0.358$
433.5	322.6	211.1	50.61	
561.3	441.8	322.6	63.04	
618.9	528.4	441.8	75.08	

TABLE XXX

Run 21a

Adsorption of Nitrogen by Spheron 6 Carbon Black

$P_1$	$P_2$	$P_0$	$\sum \frac{V_A}{W_S}$	Constants
20.4	1.6	0.0	12.11	$T_B = 298.5$ $V_T = 243$
15.0	5.0	1.6	17.05	
15.2	8.9	5.0	19.14	$T_S = 78.7$ $V_S = 53.1$
27.6	17.2	8.9	21.49	
38.1	27.2	17.2	23.20	$T_E = 280$ $V_E = 3.5$
49.4	37.9	27.2	24.91	
81.4	59.5	37.9	27.45	$W_S = 0.421$
96.3	78.2	59.5	29.05	
129.8	104.5	78.2	31.20	

TABLE XXXI

Run 21b

Adsorption of Nitrogen by Spheron 6 Carbon Black

$P_1$	$P_2$	$P_0$	$\sum \frac{V_A}{W_S}$	Constants
53.6	13.8	0.0	19.62	$T_B = 299.5$ $V_T = 243$
110.3	62.8	13.8	24.30	
172.1	119.8	62.8	27.77	$T_S = 80.6$ $V_S = 53.1$
307.4	217.6	119.8	33.76	
418.7	322.4	217.6	40.24	$T_E = 280$ $V_E = 3.5$
500.6	415.0	322.4	46.32	
620.9	520.8	415.0	54.85	$W_S = 0.421$



TABLE XXXII

Run 22

Adsorption of Nitrogen by Halloysite, -80+100 Mesh

$P_1$	$P_2$	$P_0$	$\sum \frac{V_A}{W_S}$	Constants
20.5	5.3	0.0	1.21	$T_B = 302.3$ $V_T = 249.7$
35.6	20.1	5.3	1.53	
49.9	35.5	20.1	1.67	$T_S = 78.4$ $V_S = 54.5$
78.4	57.8	35.5	1.84	
113.5	87.0	57.8	2.01	$T_E = 280$ $V_E = 3.5$
				$W_S = 2.610$ $P_S = 863$

TABLE XXXIII

Run 23

Adsorption of Nitrogen by Halloysite, -120+140 Mesh

$P_1$	$P_2$	$P_0$	$\sum \frac{V_A}{W_S}$	Constants
28.2	7.9	0.0	1.33	$T_B = 301$ $V_T = 249.7$
44.2	26.0	7.9	1.63	
76.2	52.2	26.0	1.83	$T_S = 79.5$ $V_S = 54.1$
141.6	99.3	52.2	2.12	
208.5	156.8	99.3	2.48	$T_E = 280$ $V_E = 3.5$
				$W_S = 3.085$ $P_S = 978$

TABLE XXXIV

Run 24

Adsorption of Nitrogen by Halloysite, -170+200 Mesh

$P_1$	$P_2$	$P_0$	$\sum \frac{V_A}{W_S}$	Constants
24.4	6.3	0.0	1.37	$T_B = 302$ $V_T = 249.7$
51.2	28.8	6.3	1.72	
92.6	61.9	28.8	1.99	$T_S = 79.0$ $V_S = 54.7$
125.9	95.5	61.9	2.19	
194.6	147.6	95.5	2.47	$T_E = 280$ $V_E = 3.5$
276.8	214.8	147.6	2.99	$W_S = 2.750$ $P_S = 924$

TABLE XXXV

Run 25

Adsorption of Nitrogen by Halloysite, -250+270 Mesh

$P_1$	$P_2$	$P_0$	$\sum \frac{V_A}{W_S}$	Constants
17.9	4.5	0.0	1.40	$T_B = 300$ $V_T = 249.7$
41.0	22.7	4.5	1.78	
73.9	49.4	22.7	2.00	$T_S = 78.8$ $V_S = 55.6$
115.7	84.2	49.4	2.21	
				$T_E = 280$ $V_E = 3.5$
				$W_S = 2.030$ $P_S = 902$

TABLE XXXVI

Run 26

Adsorption of Nitrogen by Halloysite, -270+325 Mesh

$P_1$	$P_2$	$P_0$	$\sum \frac{V_A}{W_S}$	Constants
20.3	8.0	0.0	1.72	$T_B = 302 \quad V_T = 249.7$
63.0	36.9	8.0	2.15	
94.8	67.6	36.9	2.43	$T_S = 79.5 \quad V_S = 55.3$
131.6	101.6	67.6	2.72	
197.5	152.5	101.6	3.16	$T_E = 280 \quad V_E = 3.5$
				$W_S = 0.940 \quad P_S = 978$

TABLE XXXVII

Run 27

Adsorption of Nitrogen by Halloysite No. 10

$P_1$	$P_2$	$P_0$	$\sum \frac{V_A}{W_S}$	Constants
23.5	11.2	0.0	1.91	$T_B = 302.8 \quad V_T = 251.4$
55.8	34.5	11.2	2.71	
108.2	73.2	34.5	3.75	$T_S = 78.3 \quad V_S = 54.7$
135.5	105.8	73.2	4.78	
203.8	157.3	105.8	6.11	$T_E = 260 \quad V_E = 5.8$
311.3	238.1	157.3	8.37	$W_S = 0.402 \quad P_S = 854$

TABLE XXXVIII

Run 28

Adsorption of Nitrogen by No. 18 Glass Beads

$P_1$	$P_2$	$P_0$	$\sum \frac{V_A}{W_S}$	Constants
13.0	4.2	0.0	0.008	$T_B = 301.5 \quad V_T = 101.4$
23.9	9.9	4.2	0.043	
51.1	22.5	9.9	0.093	$T_S = 78.2 \quad V_S = 48.8$
74.4	37.7	22.5	0.177	
100.8	56.2	37.7	0.279	$T_E = 260 \quad V_E = 5.8$
146.2	82.2	56.2	0.437	
232.3	125.4	82.2	0.707	$W_S = 10.71 \quad P_S = 844$
305.9	179.0	125.4	0.976	

TABLE XXXIX

Run 29

Adsorption of Nitrogen by Mica 432

$P_1$	$P_2$	$P_0$	$\sum \frac{V_A}{W_S}$	Constants
15.5	2.3	0.0	0.428	$T_B = 304 \quad V_T = 51.4$
30.1	7.2	2.3	0.664	
54.7	16.0	7.2	0.779	$T_S = 79.0 \quad V_S = 55.6$
93.3	30.4	16.0	0.917	
141.0	51.2	30.4	0.985	$T_E = 260 \quad V_E = 5.8$
196.3	78.4	51.2	1.130	
243.0	109.1	78.4	1.400	$W_S = 0.470 \quad P_S = 924$
280.6	141.3	109.1	1.540	

TABLE XL

Run 30a

Adsorption of Ethane by No. 18 Glass Beads

$P_1$	$P_2$	$P_0$	$\sum \frac{V_A}{W_S} \times 10^3$	$\frac{P_2}{P_S}$	Constants
0.778	0.004	0.0005	0.71	0.0	$V_3 = 390.0$
28.95	5.71	0.004	21.71	0.640	$V_5 = 0.7$
2.25	4.18	5.71	20.02	0.469	$V_6 = 1.2$
0.906	3.01	4.18	18.16	0.337	$V_8 = 0.8$
0.515	2.38	3.01	16.475	0.267	$V_{10} = 20.5$
0.071	1.82	2.38	14.90	0.204	$T_1 = 302.0$
0.025	1.41	1.82	13.65	0.158	$T_5 = 90$
0.016	1.13	1.41	12.65	0.127	$T_6 = 180$
					$P_S = 8.92$
					$W_S = 0.5052$

Sample evacuated at 230°C to 0.1 micron, then at room temperature to 0.001 micron.

TABLE XLI

Run 30b

Adsorption of Ethane by No. 18 Glass Beads

$P_1$	$P_2$	$P_0$	$\sum \frac{V_A}{W_S} \times 10^3$	$\frac{P_2}{P_S}$	Constants
2.57	0.03	0.0005	2.340	0.0036	$V_3 = 390.0$
1.09	0.05	0.03	3.300	0.0059	$V_5 = 0.7$
1.97	0.19	0.05	4.935	0.023	$V_6 = 0.9$
2.95	0.48	0.19	7.195	0.057	$V_8 = 0.8$
3.58	0.91	0.48	9.626	0.108	$V_{10} = 20.8$
5.18	1.84	0.91	12.649	0.218	$T_1 = 301$
8.56	3.07	1.84	17.625	0.365	$T_5 = 90$
0.58	1.95	3.07	16.423	0.231	$T_6 = 180$
					$P_S = 8.44$
					$W_S = 0.5052$

Sample evacuated at room temperature (2 hours) to less than 0.001 micron after run 30a.



TABLE XLII

Run 31

Adsorption of Ethane by Mica 432

$P_1$	$P_2$	$P_0$	$\sum \frac{V_A}{W_S} \times 10^3$	$\frac{P_2}{P_S}$	Constants
2.20	0.06	0.0	102.1	0.007	$V_3 = 390.0$
2.45	0.09	0.06	214.9	0.011	$V_5 = 0.7$
4.70	0.24	0.09	427.7	0.028	$V_6 = 0.7$
6.36	0.64	0.24	700.0	0.075	$V_8 = 0.8$
10.41	2.25	0.64	1085	0.264	$V_{10} = 20.7$
8.51	3.33	2.25	1329	0.391	$T_1 = 302$
					$T_5 = 90$
					$T_6 = 180$
					$P_S = 8.52$
					$W_S = 0.0097$

Sample evacuated 8 hours at 210°C to less than 0.001 micron.

TABLE XLIII

Run 32b\*

Adsorption of Ethane by Silica 196

$P_1$	$P_2$	$P_0$	$\sum \frac{V_A}{W_S} \times 10^3$	$\frac{P_2}{P_S}$	Constants
3.48	0.60	0.0	102.2	0.062	$V_3 = 389.8$
2.34	0.96	0.60	150.9	0.100	$V_5 = 0.2$
3.37	1.84	0.96	203.6	0.191	$V_6 = 1.0$
3.91	2.59	1.84	249.0	0.269	$V_8 = 0.8$
4.755	3.26	2.59	300.8	0.339	$V_{10} = 28.4$
					$T_1 = 303$
					$T_5 = 90$
					$T_6 = 180$
					$P_S = 9.62$
					$W_S = 0.0128$

\*Run 32a is not included in tables, but is mentioned in "Discussion of Results".

Sample evacuated 45 minutes at 200°C to less than 0.001 micron after Run 32a.

## TABLES XLIV AND XLV

## Runs 33a and 33b

## Adsorption of Ethane by Halloysite No. 10

$P_1$	$P_2$	$P_0$	$\sum \frac{V_A}{W_S} \times 10^3$	$\frac{P_2}{P_S}$	Constants
Run 33a:					
5.162	0.032	0.0	98.50	0.004	$V_3 = 389.8$
6.054	0.067	0.032	213.47	0.008	$V_5 = 0.2$
11.958	0.327	0.067	436.56	0.037	$V_6 = 1.0$
8.667	0.630	0.327	590.57	0.071	$V_8 = 0.8$
10.889	1.232	0.630	775.28	0.139	$V_{10} = 23.8$
Run 33b:					
7.744		1.232			$T_1 = 302.5$
					$T_5 = 90$
					$T_6 = 180$
					$P_S = 8.88$
					$W_S = 0.0241$

Run 33a, sample evacuated 10 hours at 230°C to less than 0.001 micron. Run 33b, sample evacuated 1 hour at 230°C.

## TABLE XLVI

## Run 33c

## Adsorption of Ethane by Halloysite No. 10

$P_1$	$P_2$	$P_0$	$\sum \frac{V_A}{W_S} \times 10^3$	$\frac{P_2}{P_S}$	Constants
18.995	0.267	0.0	358.6	0.031	$V_3 = 389.8$
13.033	0.404	0.267	600.4	0.046	$V_5 = 0.2$
15.084	0.844	0.404	872.7	0.097	$V_6 = 1.0$
15.947	1.114	0.844	1156.6	0.127	$V_8 = 0.8$
22.742	1.957	1.114	1553.8	0.224	$V_{10} = 23.8$
16.020	1.881	1.957	1824.8	0.215	$T_1 = 303$
19.852	2.808	1.881	2150.2	0.321	$T_5 = 90$
26.419	4.152	2.808	2575.1	0.475	$T_6 = 180$
					$P_S = 8.74$
					$W_S = 0.0241$

Sample evacuated 15 hours at 220°C to less than 0.001 micron.

TABLE XLVII

Run 34

Adsorption of Ethane by Nickel

$P_1$	$P_2$	$P_0$	$\sum \frac{V_A}{W_S} \times 10^3$	$\frac{P_2}{P_S}$	Constants
1.578	0.022	0.0	2.096	0.003	$V_3 = 388.8$
2.687	0.039	0.022	5.667	0.004	$V_5 = 0.2$
4.729	0.189	0.039	11.778	0.022	$V_6 = 1.0$
4.610	0.341	0.189	17.523	0.039	$V_8 = 0.8$
6.084	0.592	0.341	24.908	0.067	$V_{10} = 18.8$
9.718	1.436	0.592	36.01	0.163	$T_1 = 301.5$
8.812	2.009	1.436	45.14	0.229	$T_5 = 90$
12.361	3.442	2.009	57.05	0.392	$T_6 = 180$
					$P_S = 8.79$
					$W_S = 0.3445$

Sample evacuated at 180°C for 18 hours to 0.003 micron.

TABLE XLVIII

Run 35

Adsorption of Ethane by Cadmium

$P_1$	$P_2$	$P_0$	$\sum \frac{V_A}{W_S} \times 10^3$	$\frac{P_2}{P_S}$	Constants
8.829	0.094	0.0	22.95	0.010	$V_3 = 389.8$
11.152	0.270	0.094	51.55	0.029	$V_5 = 0.2$
13.409	0.640	0.270	85.07	0.068	$V_6 = 1.0$
13.700	2.194	0.640	115.11	0.233	$V_8 = 0.8$
11.294	3.545	2.194	135.3	0.377	$V_{10} = 18.8$
					$T_1 = 301.5$
					$T_5 = 90$
					$T_6 = 180$
					$P_S = 9.40$
					$W_S = 0.1766$

Sample evacuated at 80°C for 9 hours to less than 0.001 micron.

TABLE XLIX

Run 36

Adsorption of Ethane by Halloysite -170+200 Mesh

$P_1$	$P_2$	$P_0$	$\sum \frac{V_A}{W_S} \times 10^3$	$\frac{P_2}{P_S}$	Constants
8.865	0.042	0.0	179.9	0.005	$V_3 = 389.8$
16.933	0.630	0.042	511.8	0.071	$V_5 = 0.2$
12.902	1.019	0.630	753.7	0.115	$V_6 = 1.0$
15.202	1.517	1.019	1032.2	0.171	$V_8 = 0.8$
18.338	2.052	1.517	1363.7	0.232	$V_{10} = 18.8$
					$T_1 = 302.5$
					$T_5 = 90$
					$T_6 = 180$
					$P_S = 8.848$
					$W_S = 0.0227$

Sample evacuated 12 hours at 300°C to less than 0.001 micron.

TABLE L

Run 37

Adsorption of Ethane by Halloysite -250+270 Mesh

$P_1$	$P_2$	$P_0$	$\sum \frac{V_A}{W_S} \times 10^3$	$\frac{P_2}{P_S}$	Constants
15.298	0.073	0.0	253.4	0.008	$V_3 = 389.8$
18.995	0.439	0.073	562.0	0.050	$V_5 = 0.2$
19.907	0.889	0.439	878.2	0.100	$V_6 = 1.0$
19.771	1.328	0.889	1184.8	0.150	$V_8 = 0.8$
27.143	2.035	1.328	1602.2	0.230	$V_{10} = 18.8$
31.555	2.921	2.035	2078.1	0.330	$T_1 = 303.5$
37.371	4.533	2.921	2623.3	0.512	$T_5 = 90$
41.377	5.498	4.533	3219.7	0.621	$T_6 = 180$
					$P_S = 8.85$
					$W_S = 0.0277$

Sample evacuated 14 hours at 300°C to less than 0.001 micron.

APPENDIX IV

Figures



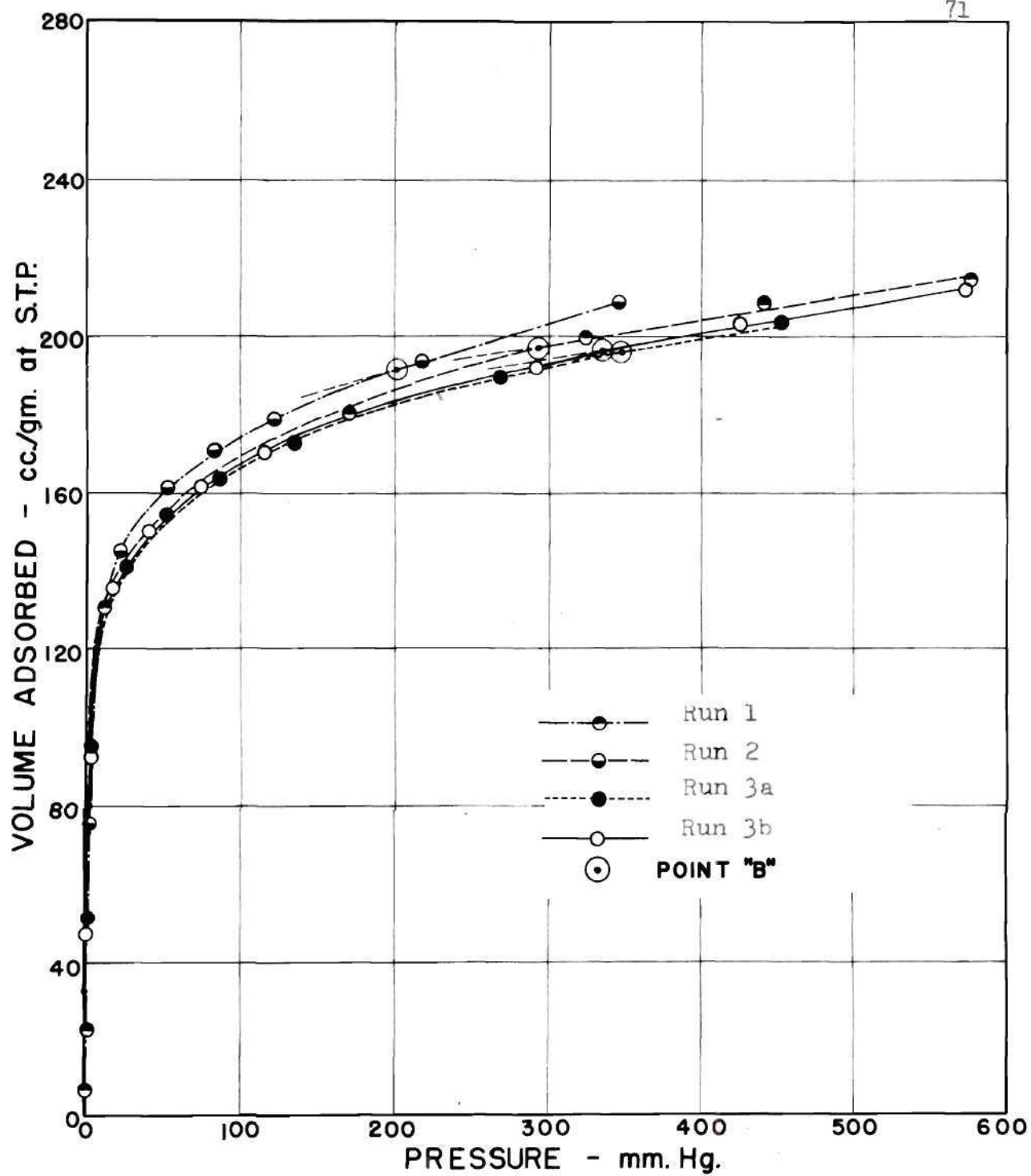


Figure 1. Adsorption of Nitrogen by Activated Charcoal

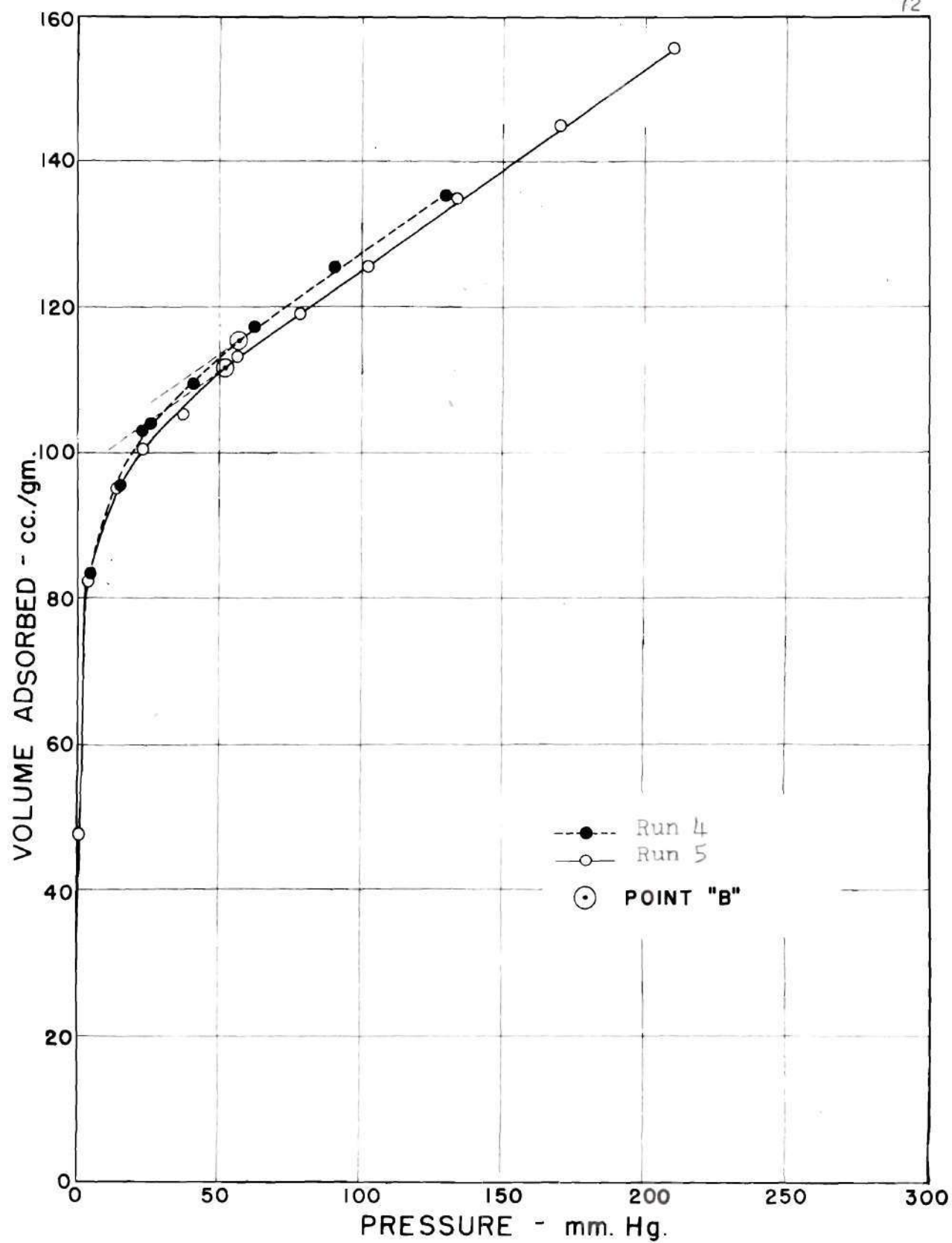


Figure 2. Adsorption of Nitrogen by Cabot Black MO-647

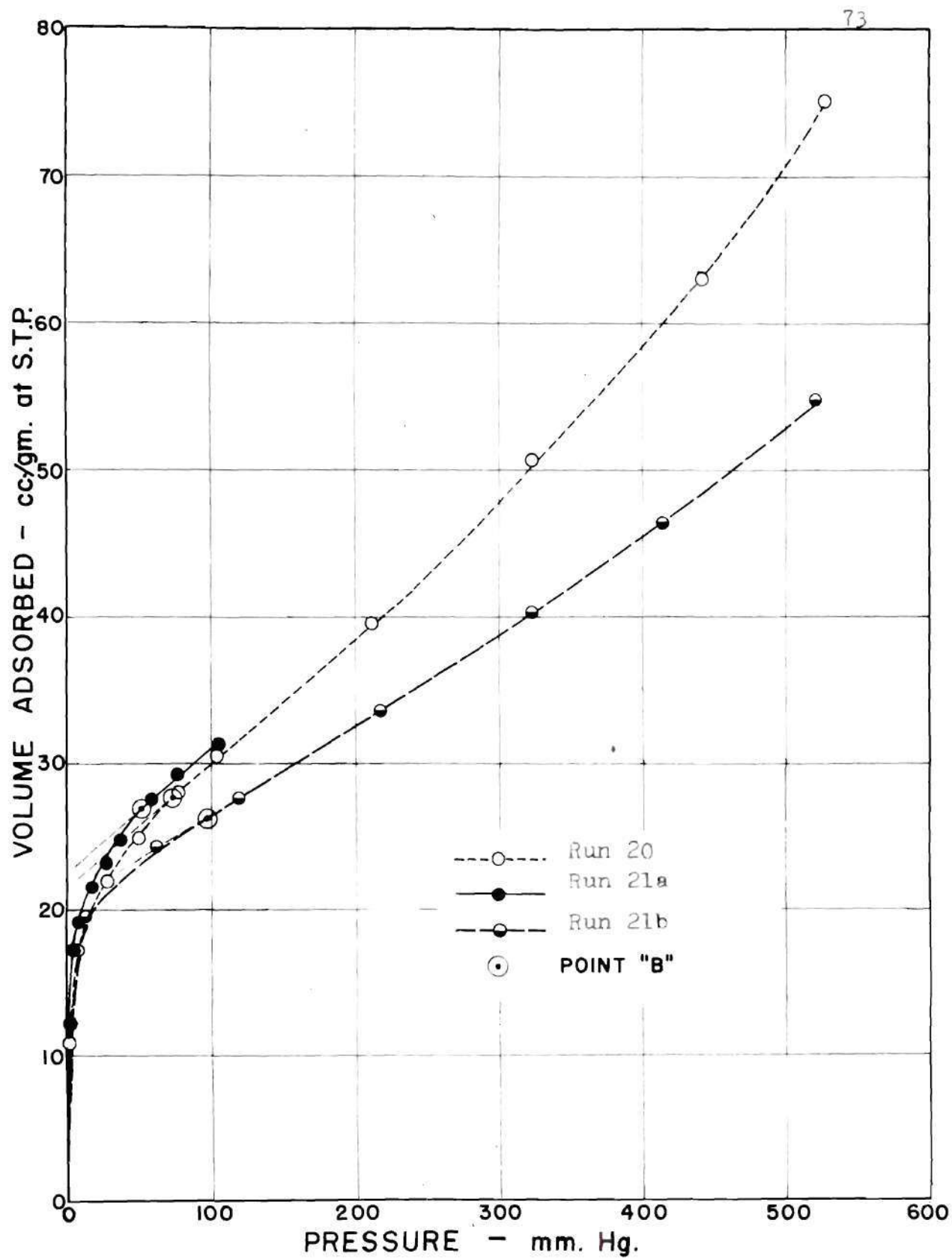


Figure 3. Adsorption of Nitrogen by Spheron 6 Carbon Black

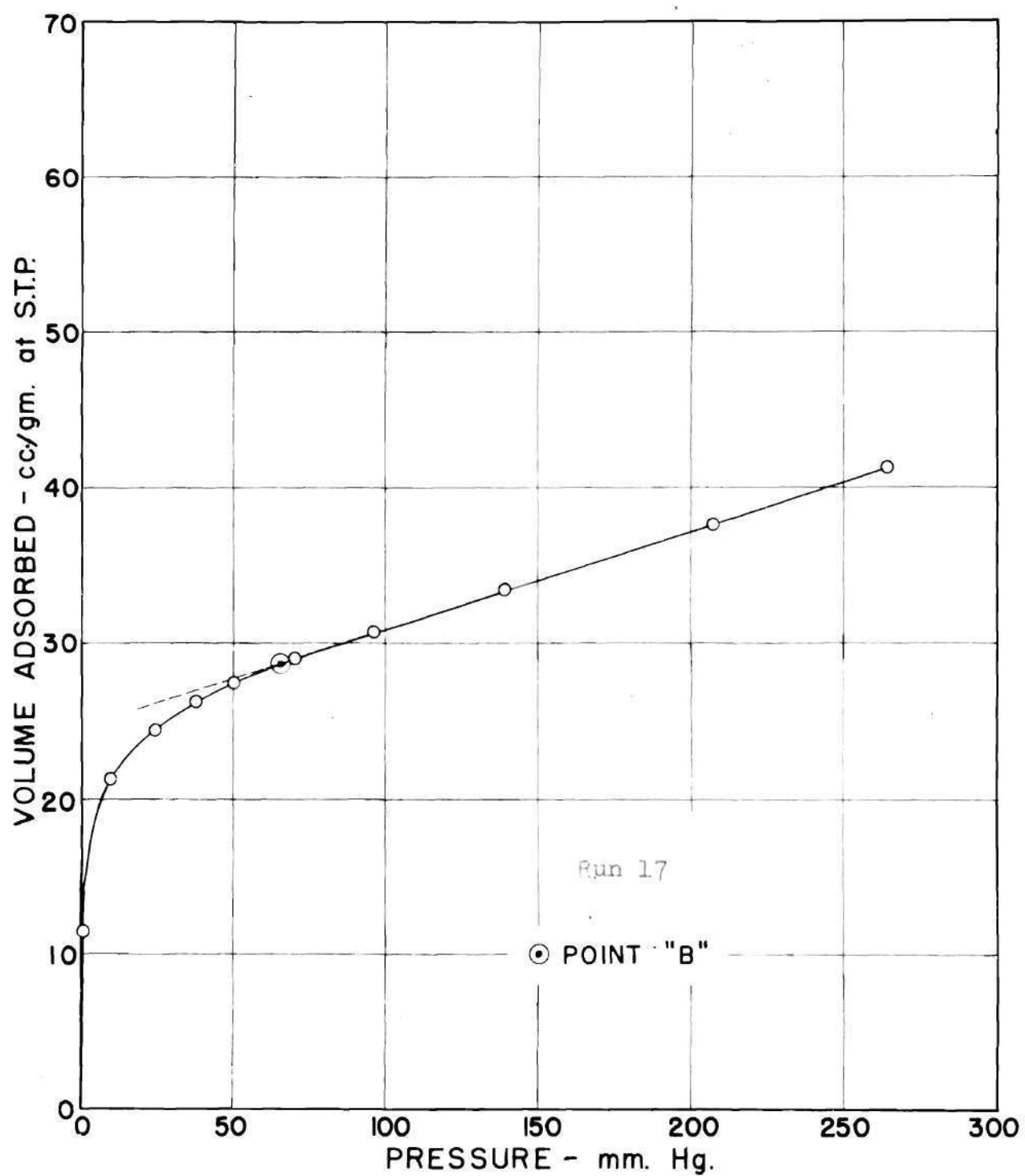


Figure 4. Adsorption of Nitrogen by Attapulugus Clay

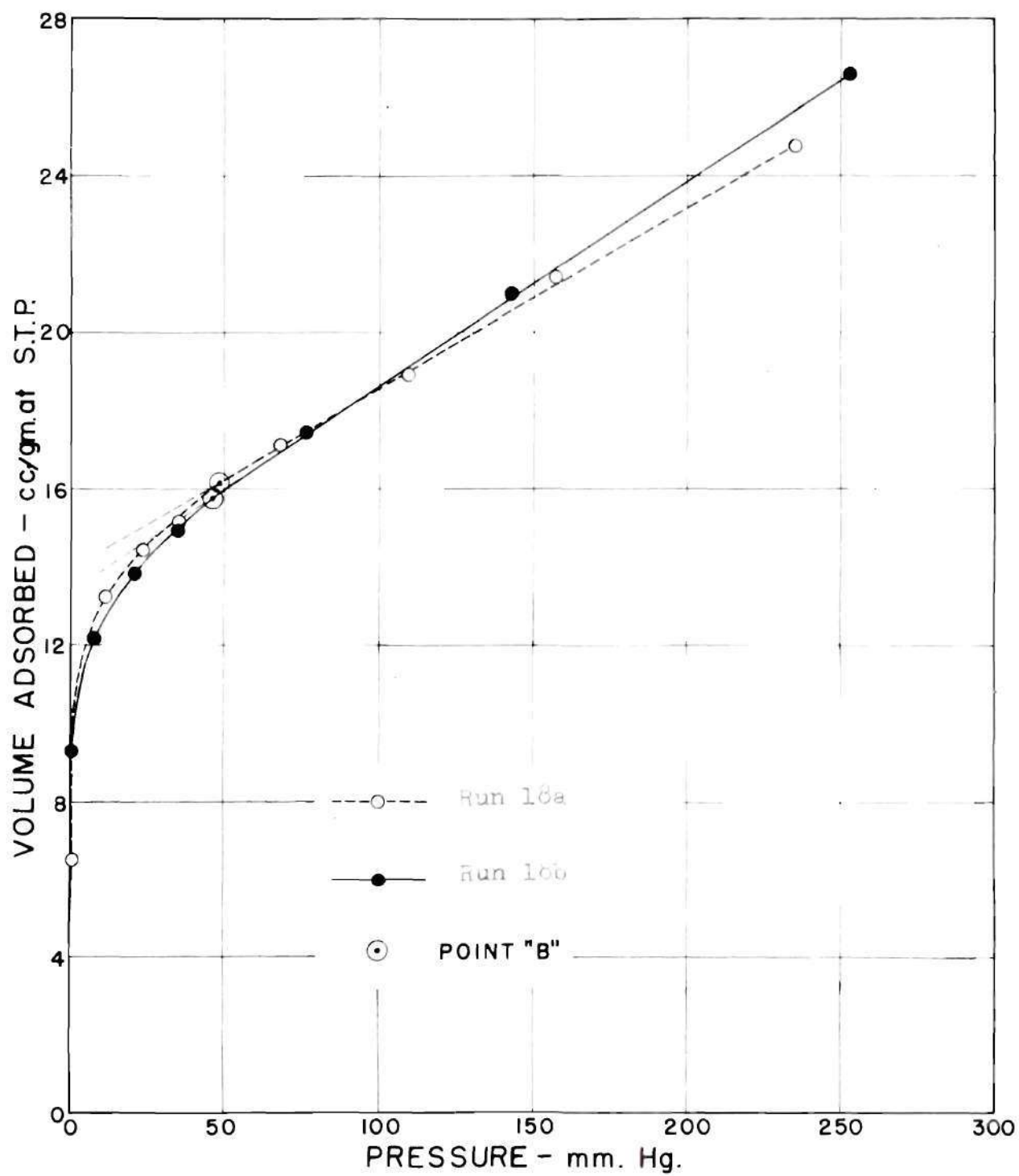


Figure 5. Adsorption of Nitrogen by Manganese Dioxide



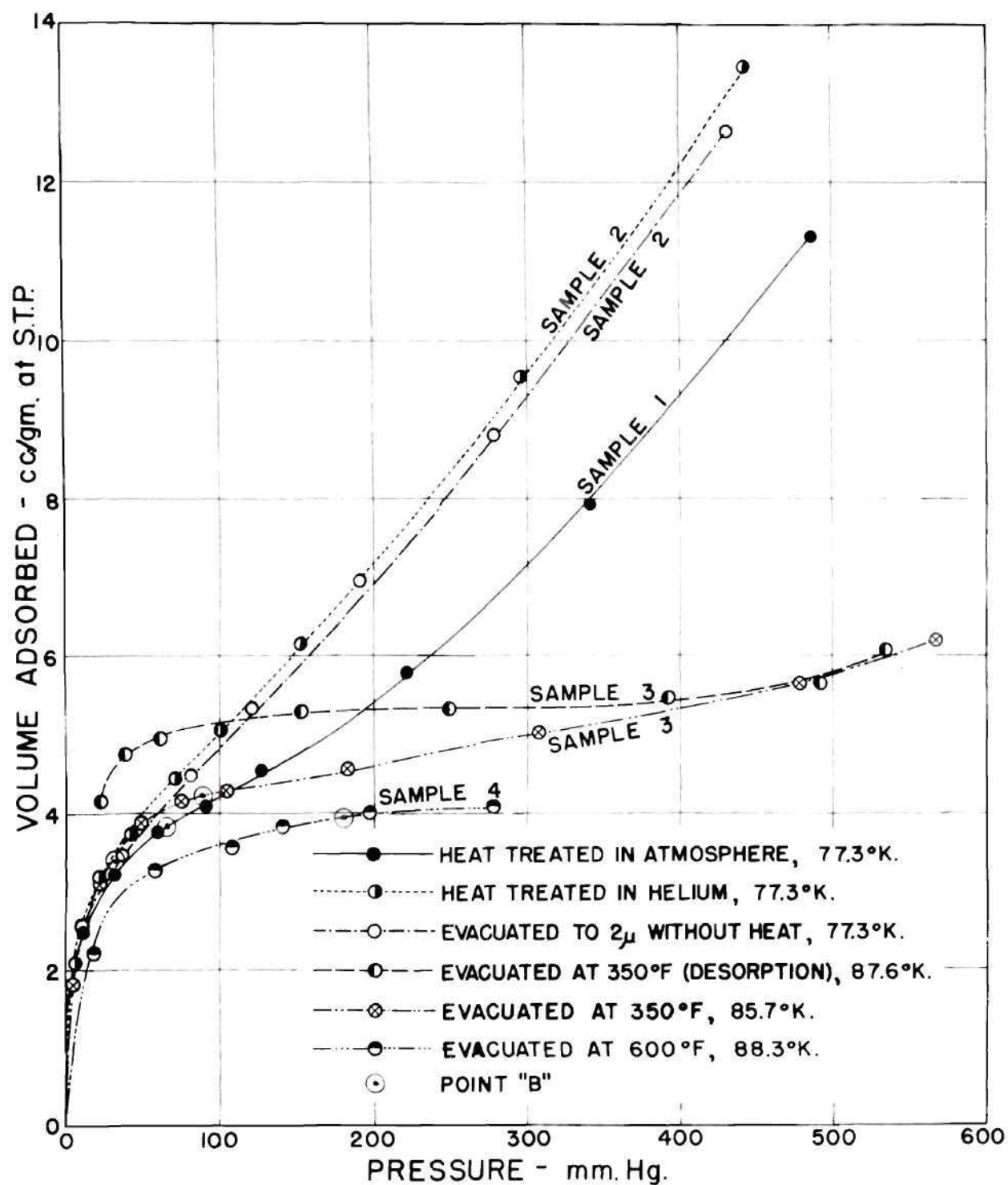


Figure 6. Adsorption of Nitrogen by Kaolinite

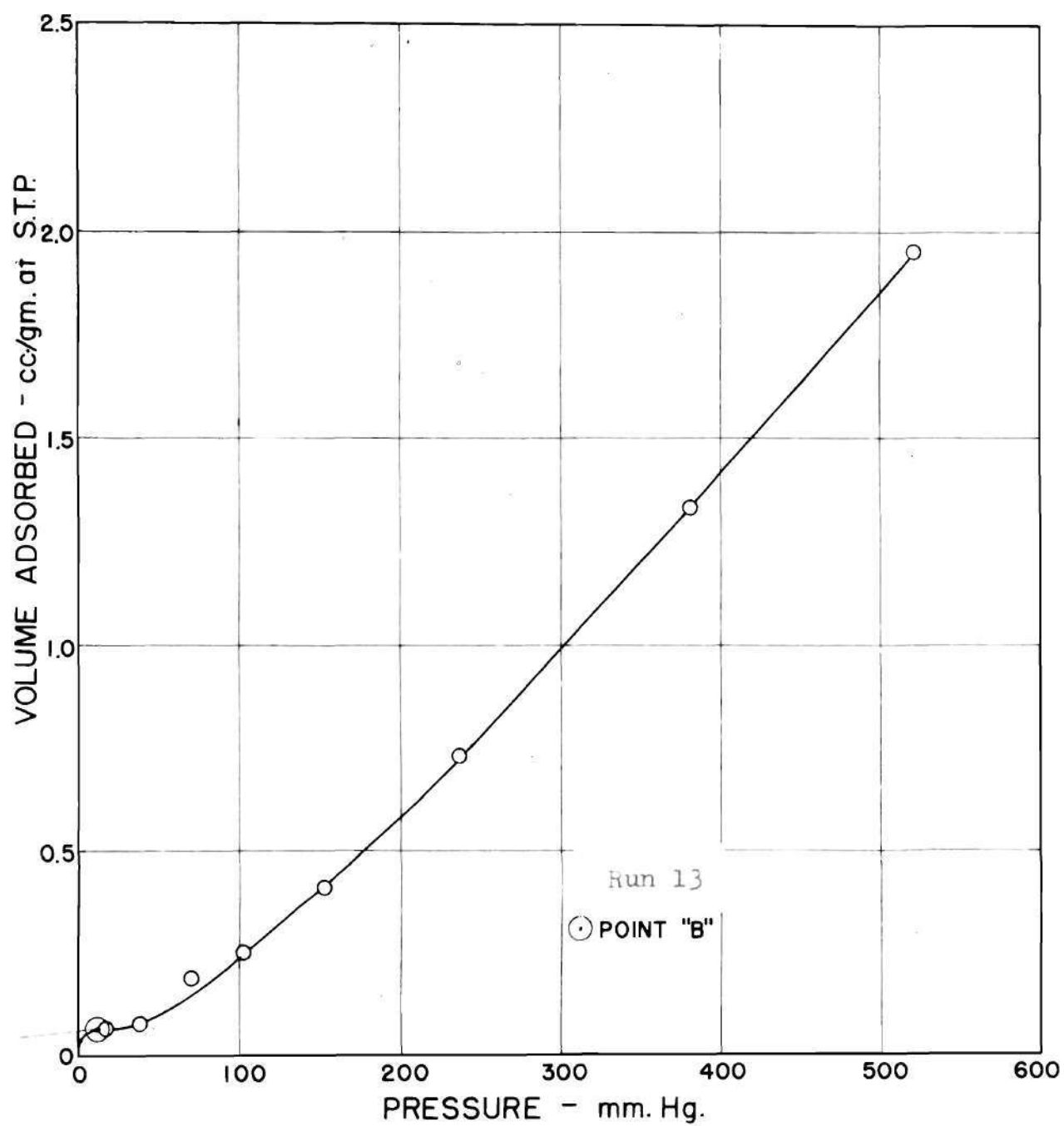


Figure 7. Adsorption of Nitrogen by Aluminum

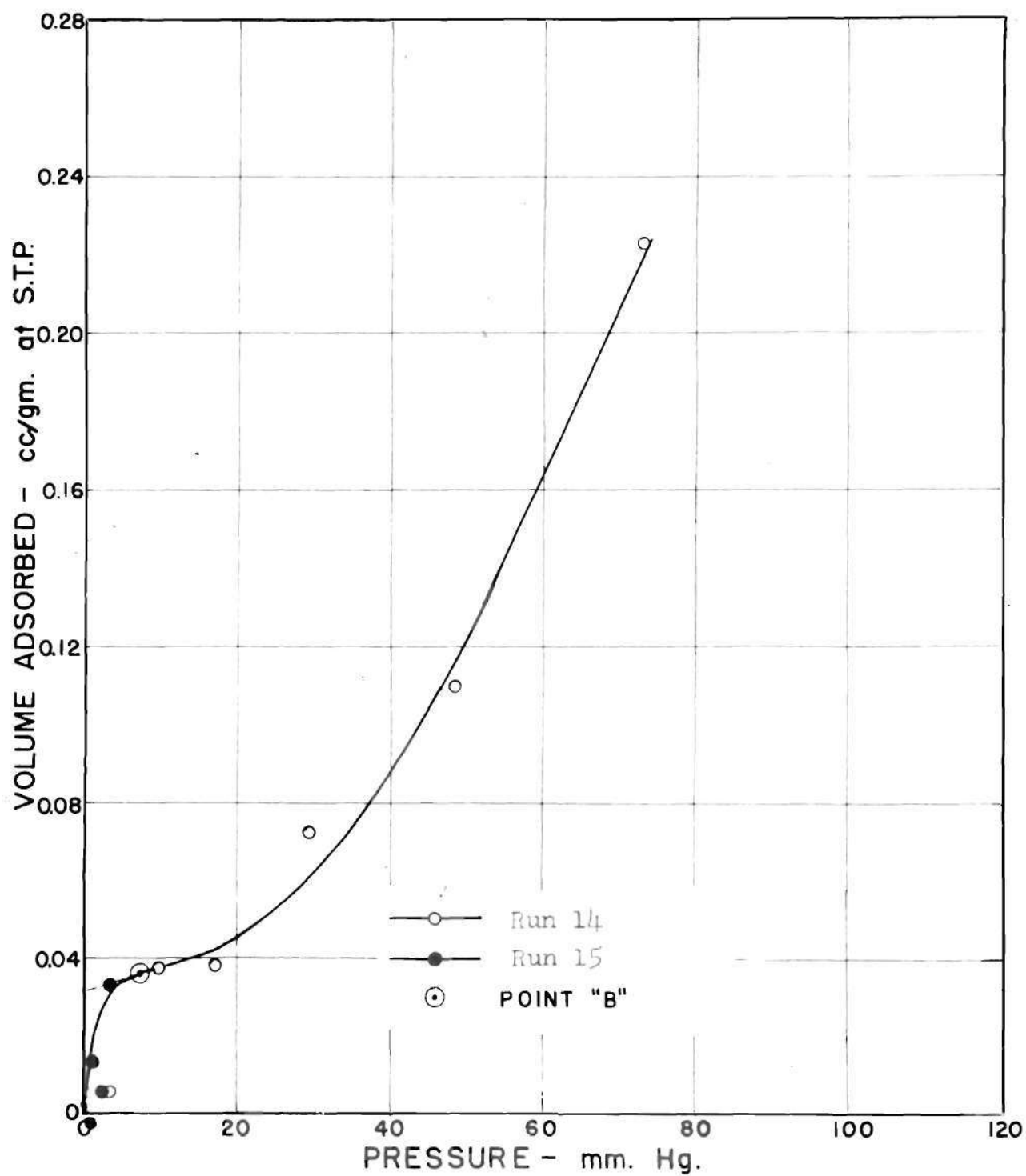


Figure 8. Adsorption of Nitrogen by 15-Micron Monofilament Nylon

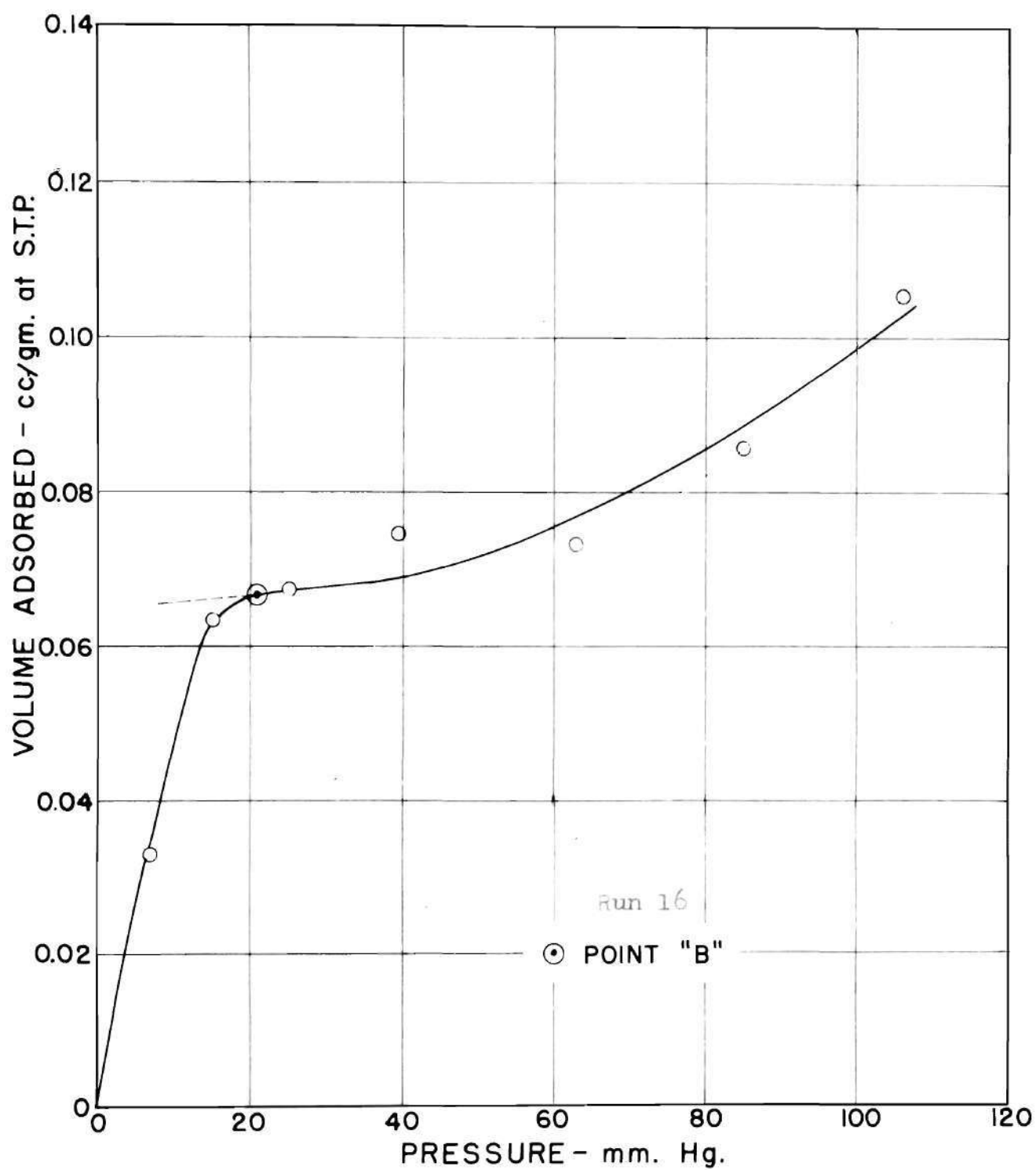


Figure 9. Adsorption of Nitrogen by Copper

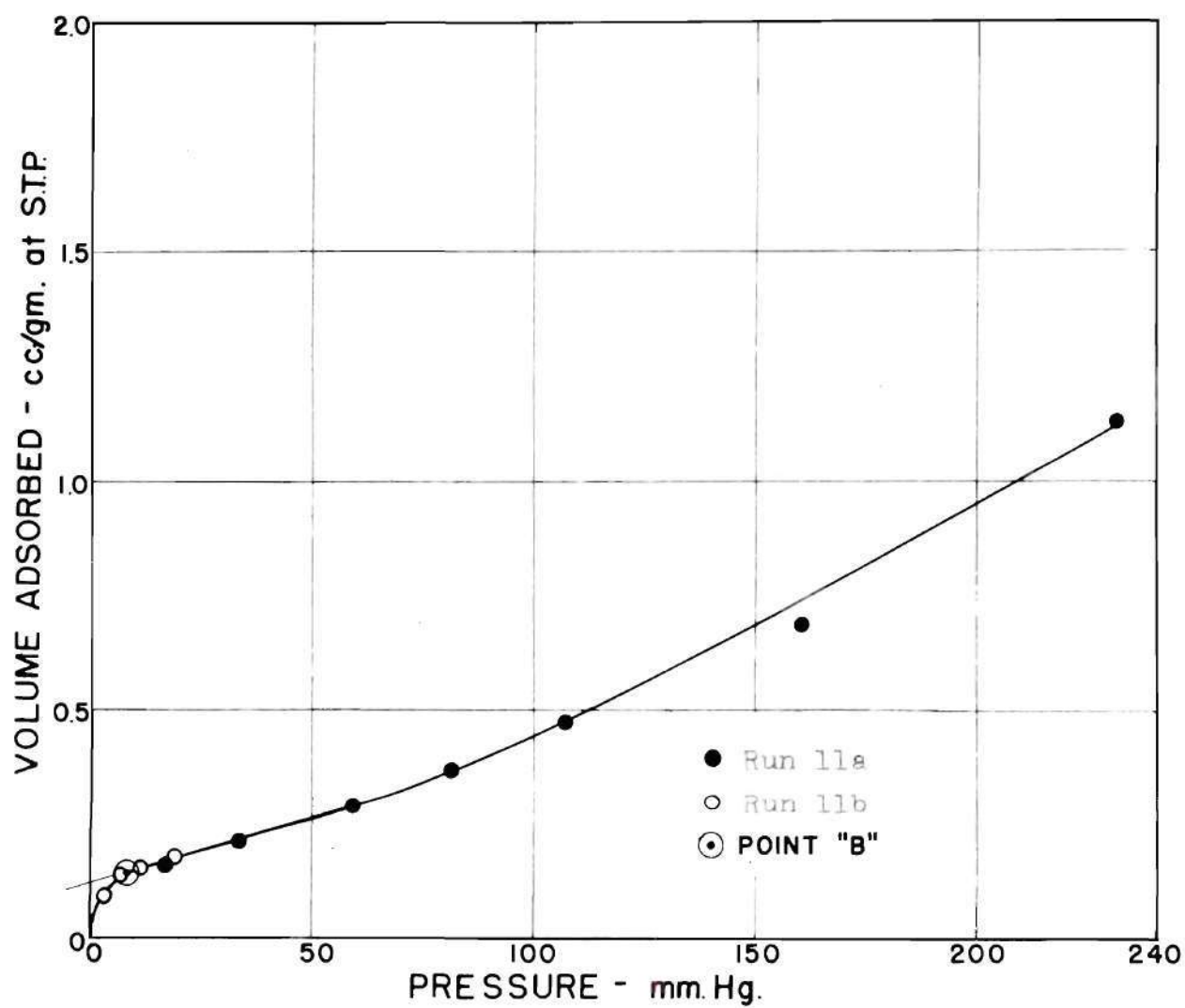


Figure 10. Adsorption of Nitrogen by Quartz Sand



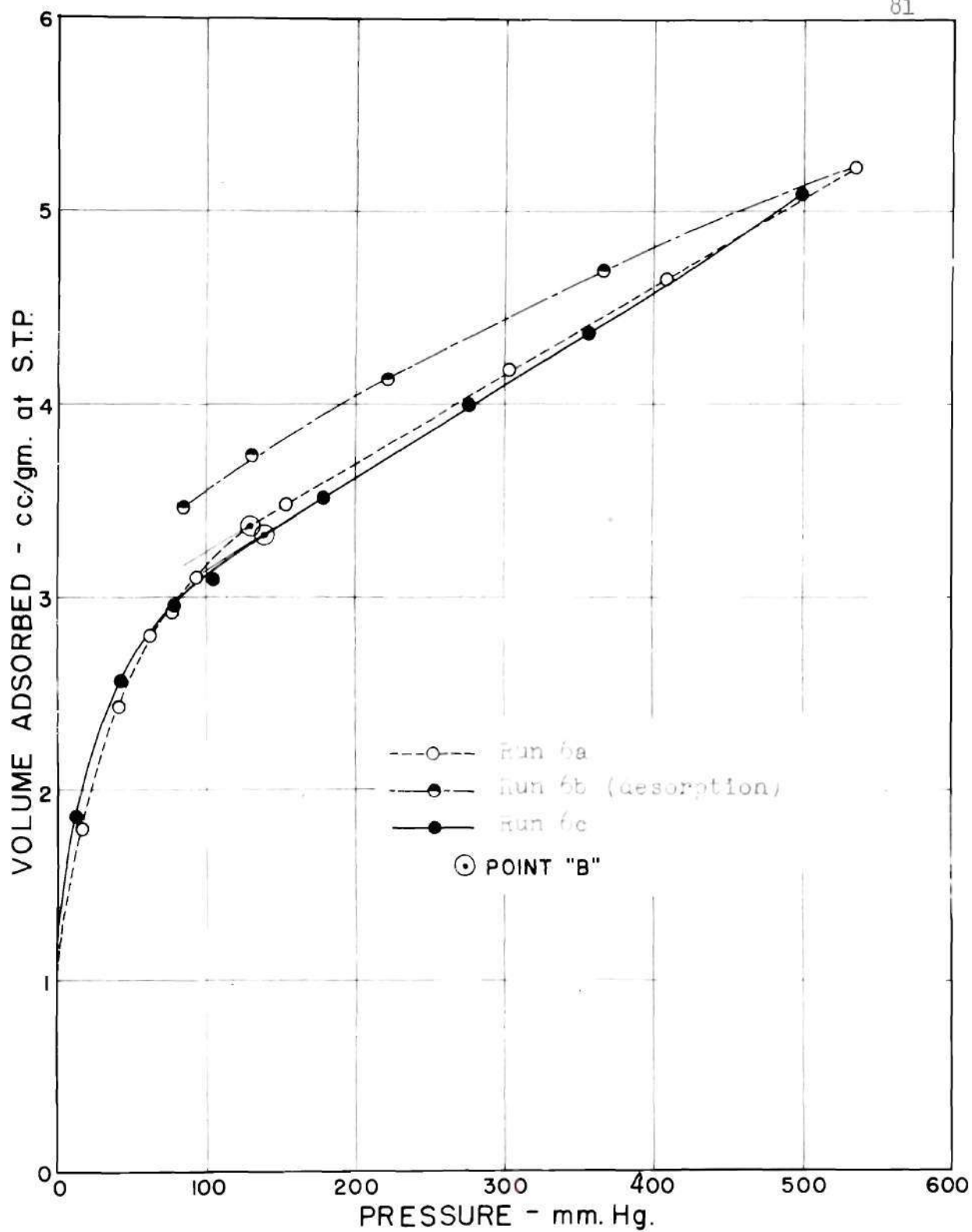


Figure 11. Adsorption of Nitrogen by Unsized Galloysite

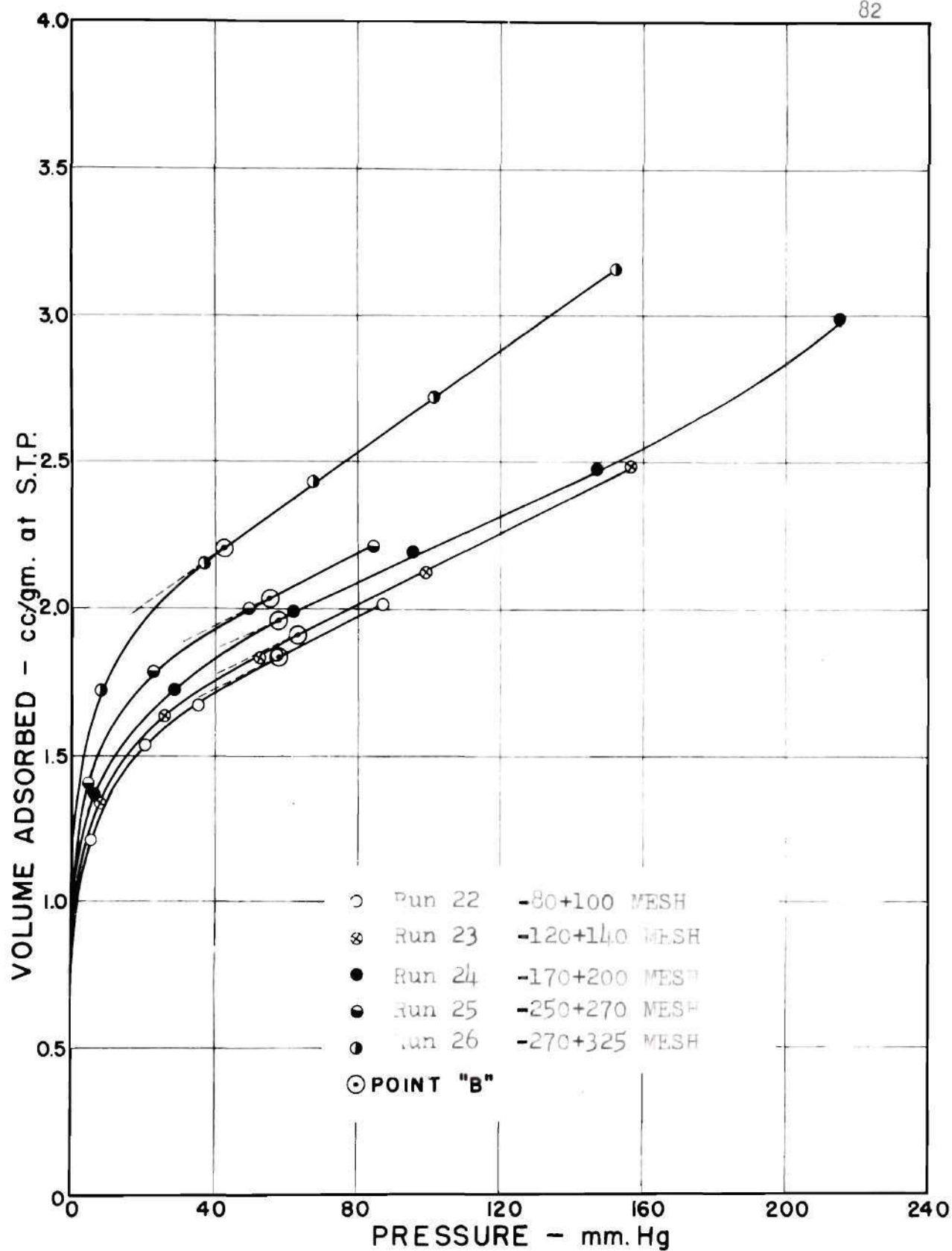


Figure 12. Adsorption of Nitrogen by Five Sized Fractions of Halloysite

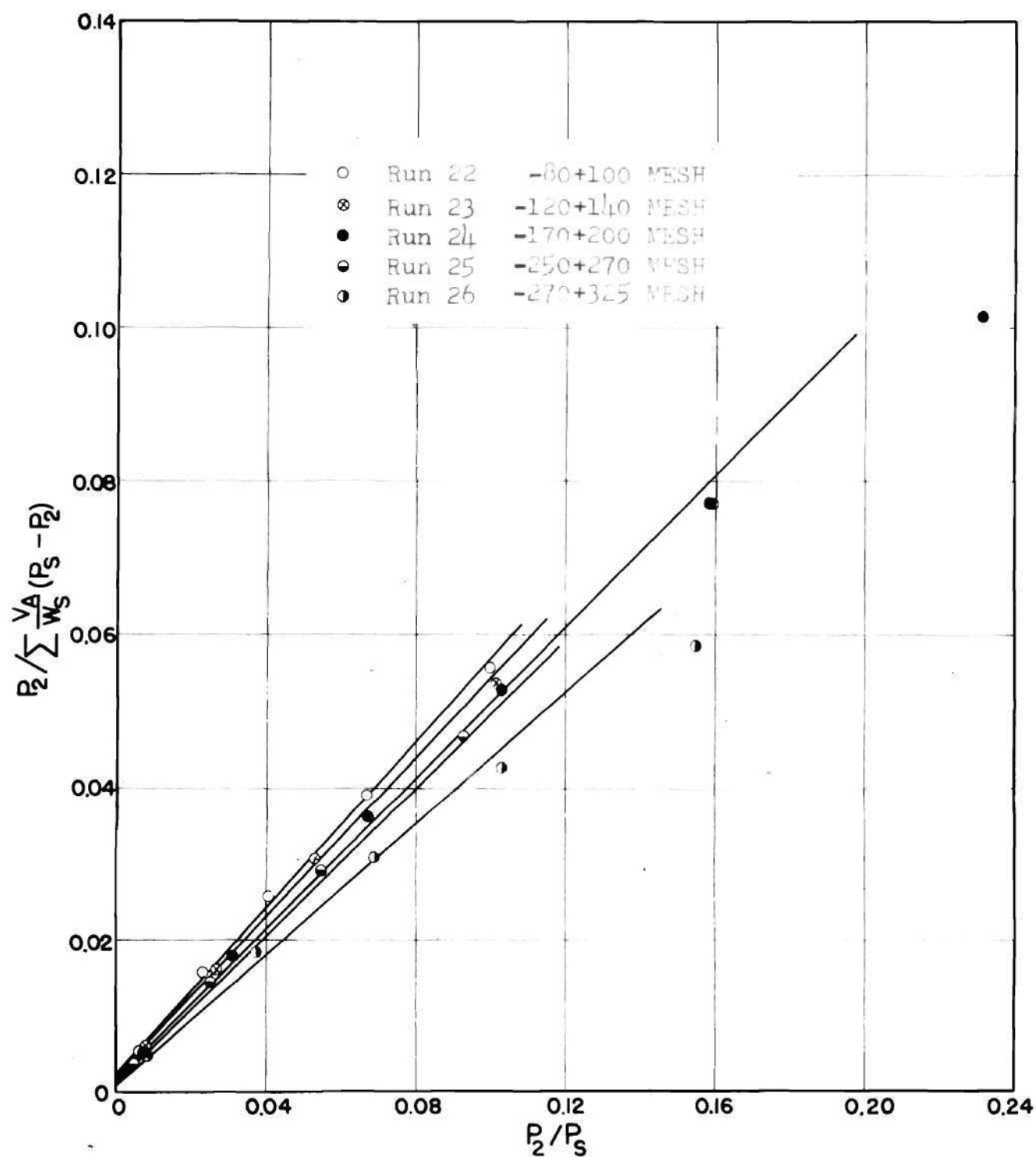


Figure 13. Graph of BET Equations for Five Sized Fractions of Halloysite

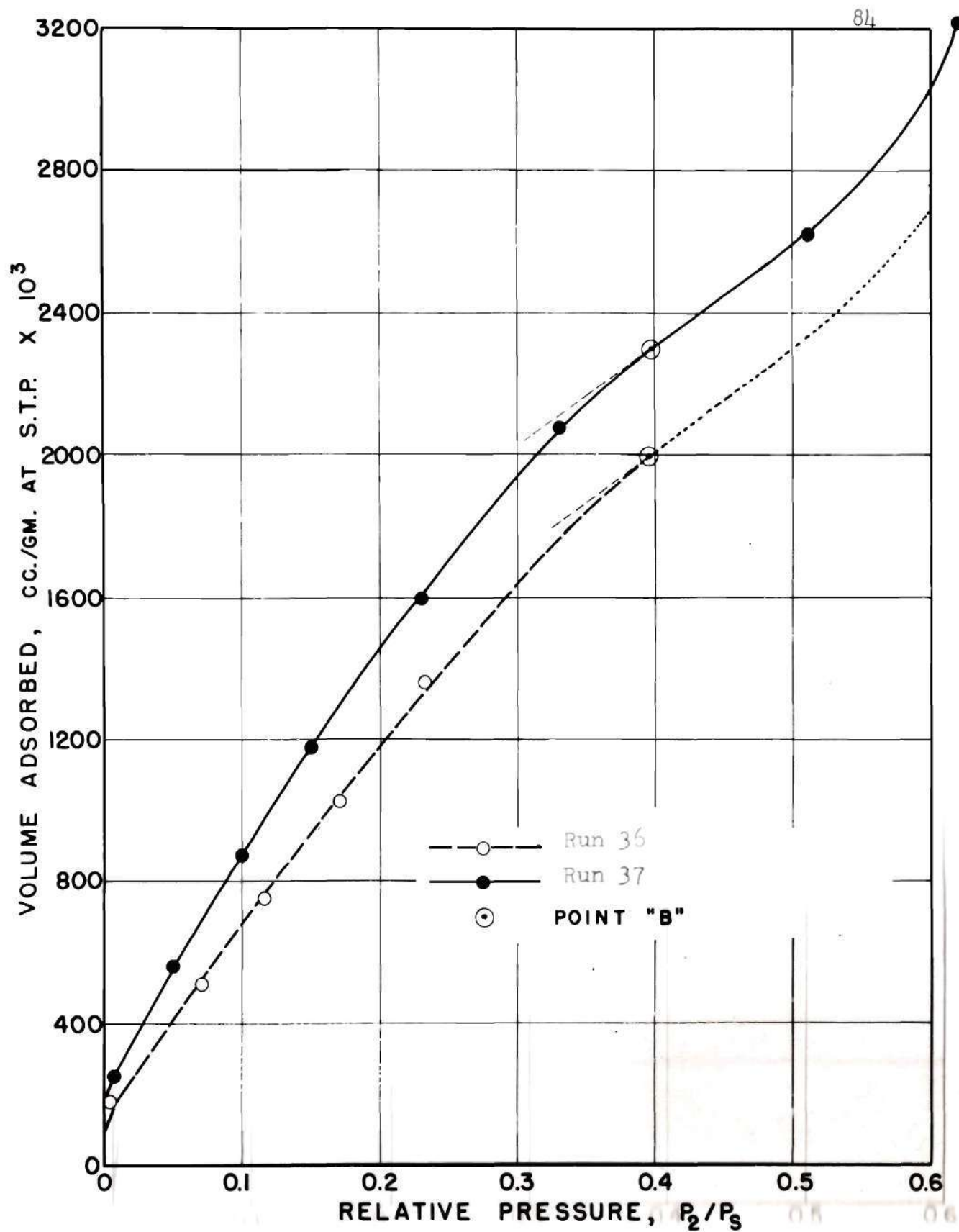


Figure 14. Adsorption of Ethane on Two Sized Fractions of Halloysite

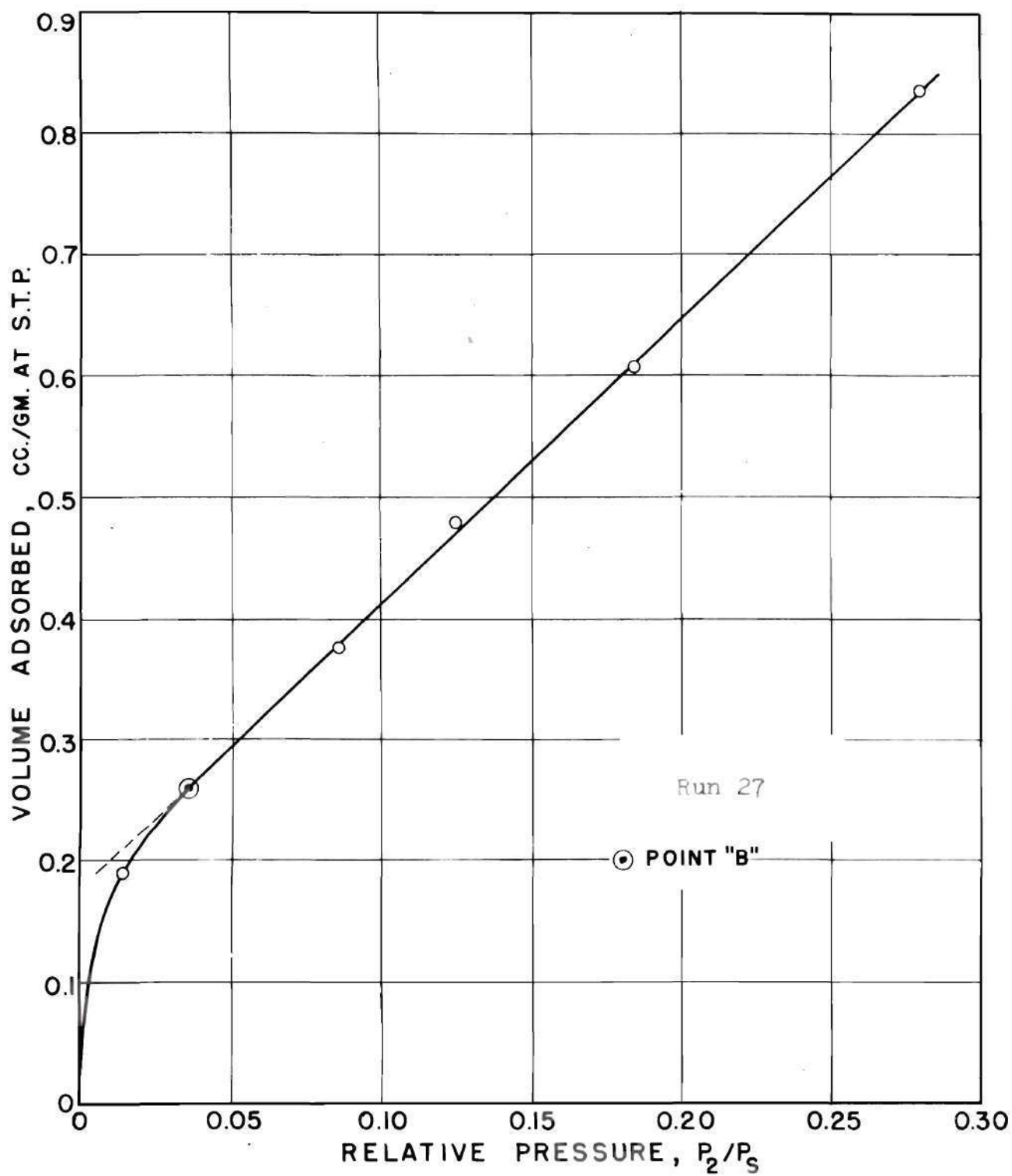


Figure 15. Adsorption of Nitrogen by Halloysite No. 10



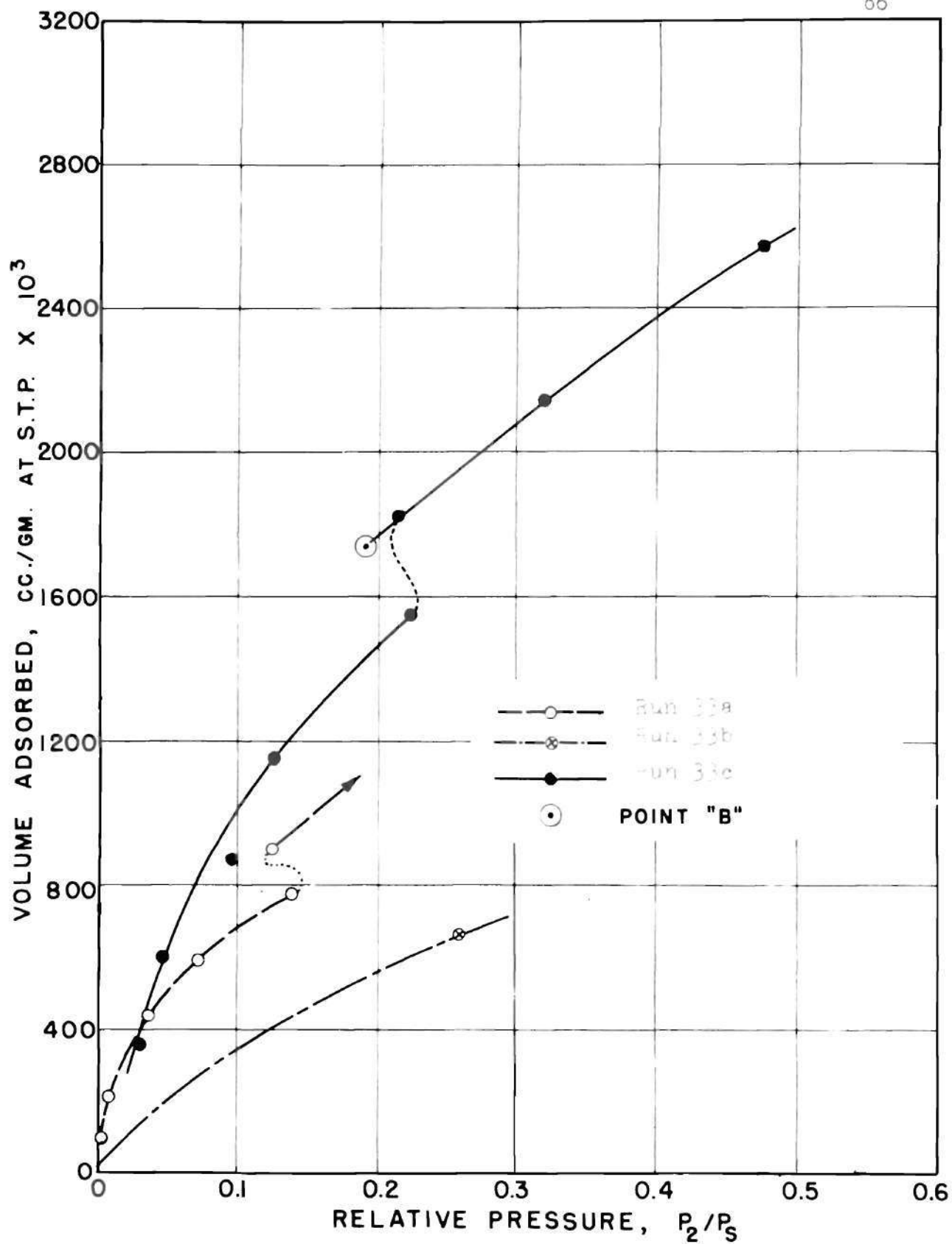


Figure 1<sup>4</sup>. Adsorption of isane by allorite No. 10

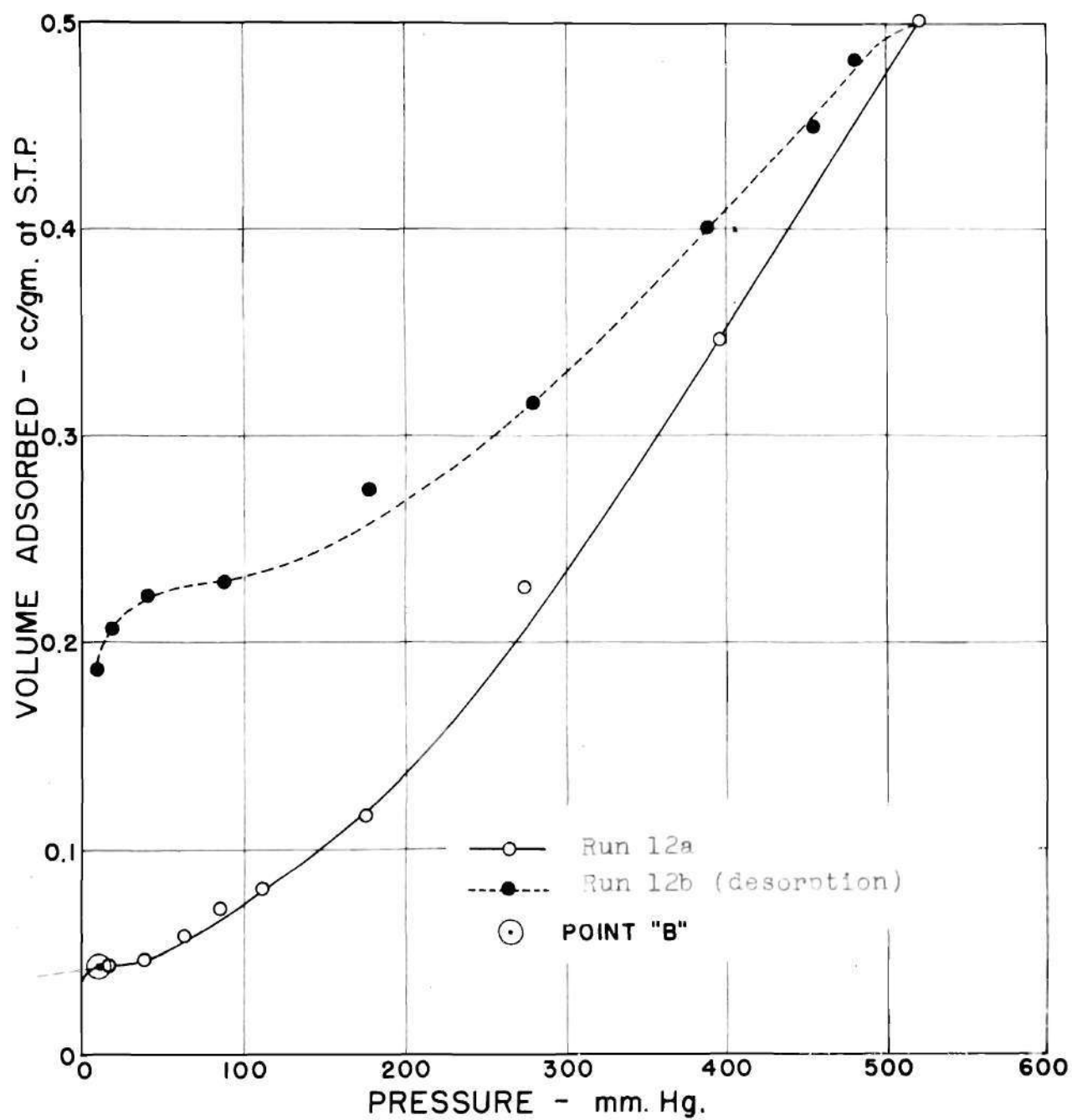


Figure 17. Adsorption of Nitrogen by Nickel

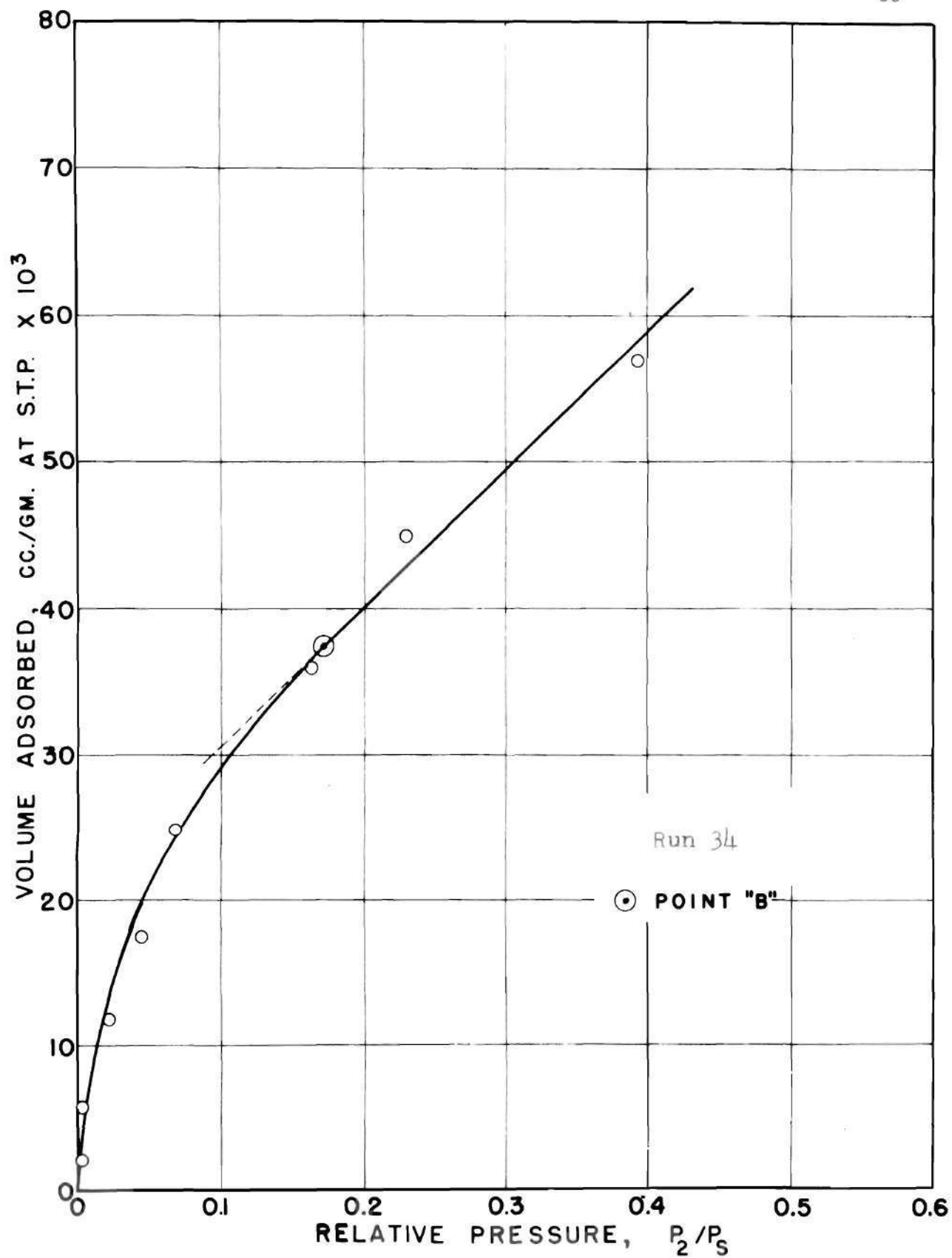


Figure 18. Adsorption of Ethane by Nickel

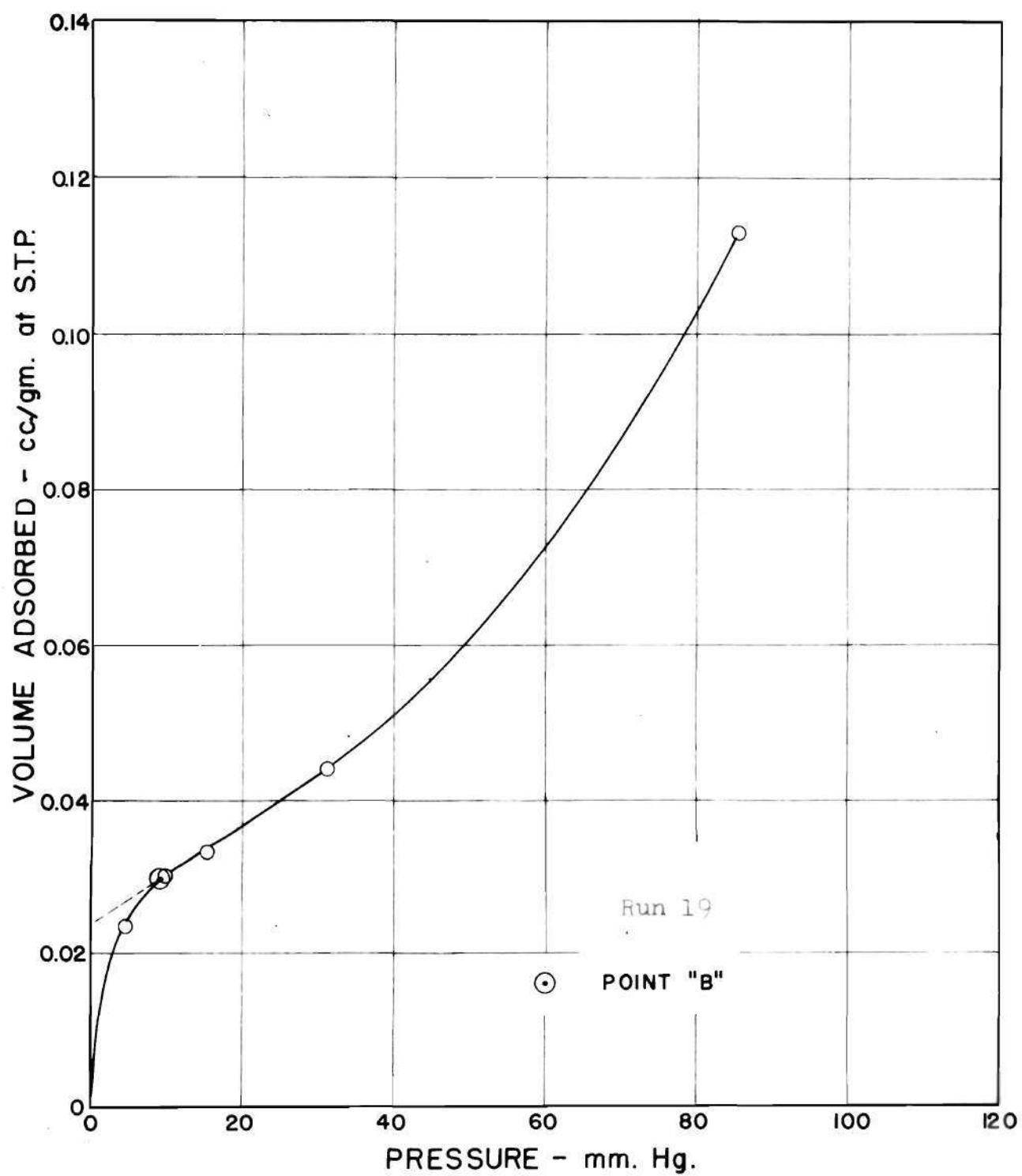


Figure 19. Adsorption of Nitrogen by Cadmium

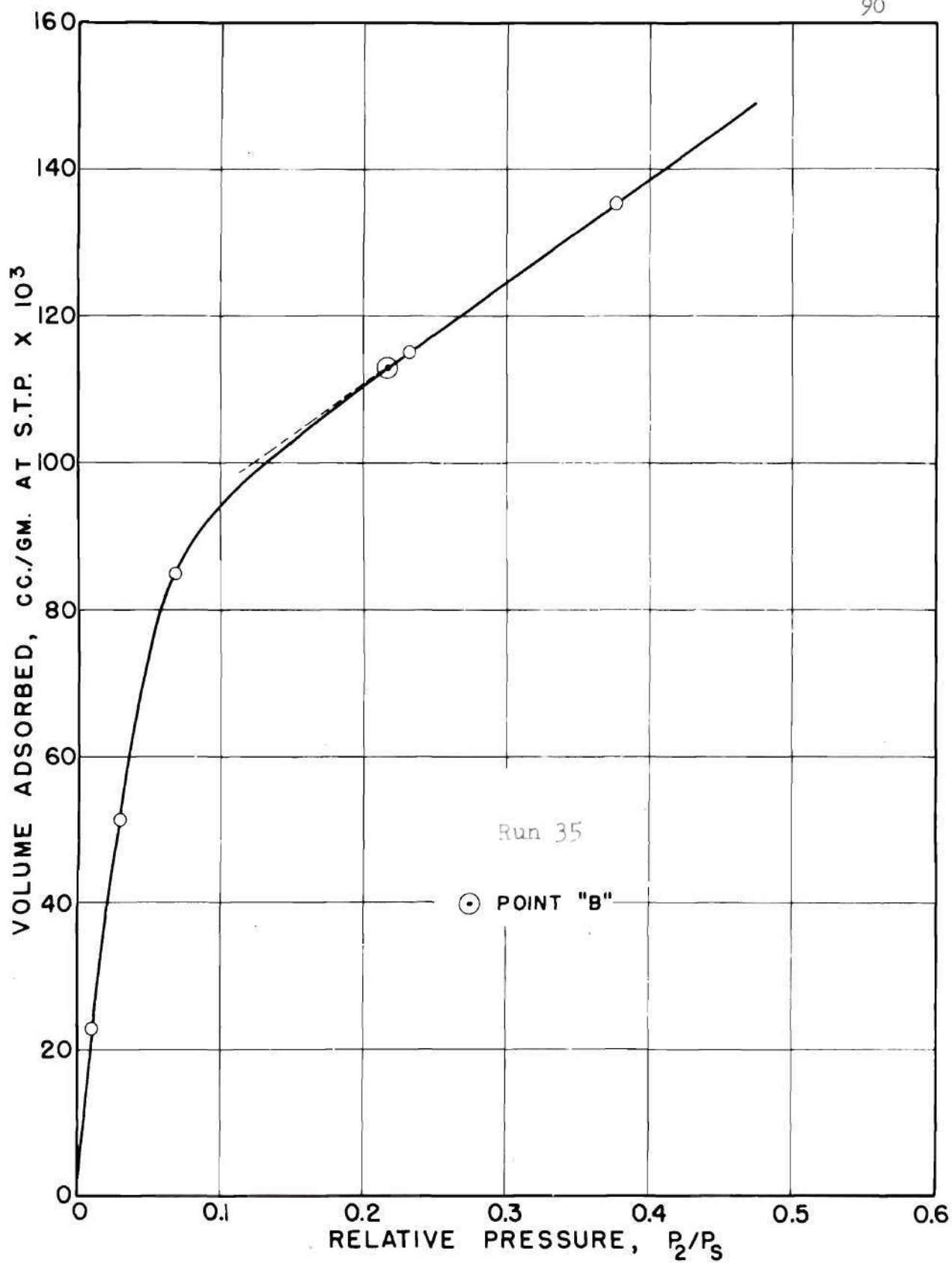


Figure 20. Adsorption of Ethane by Cadmium



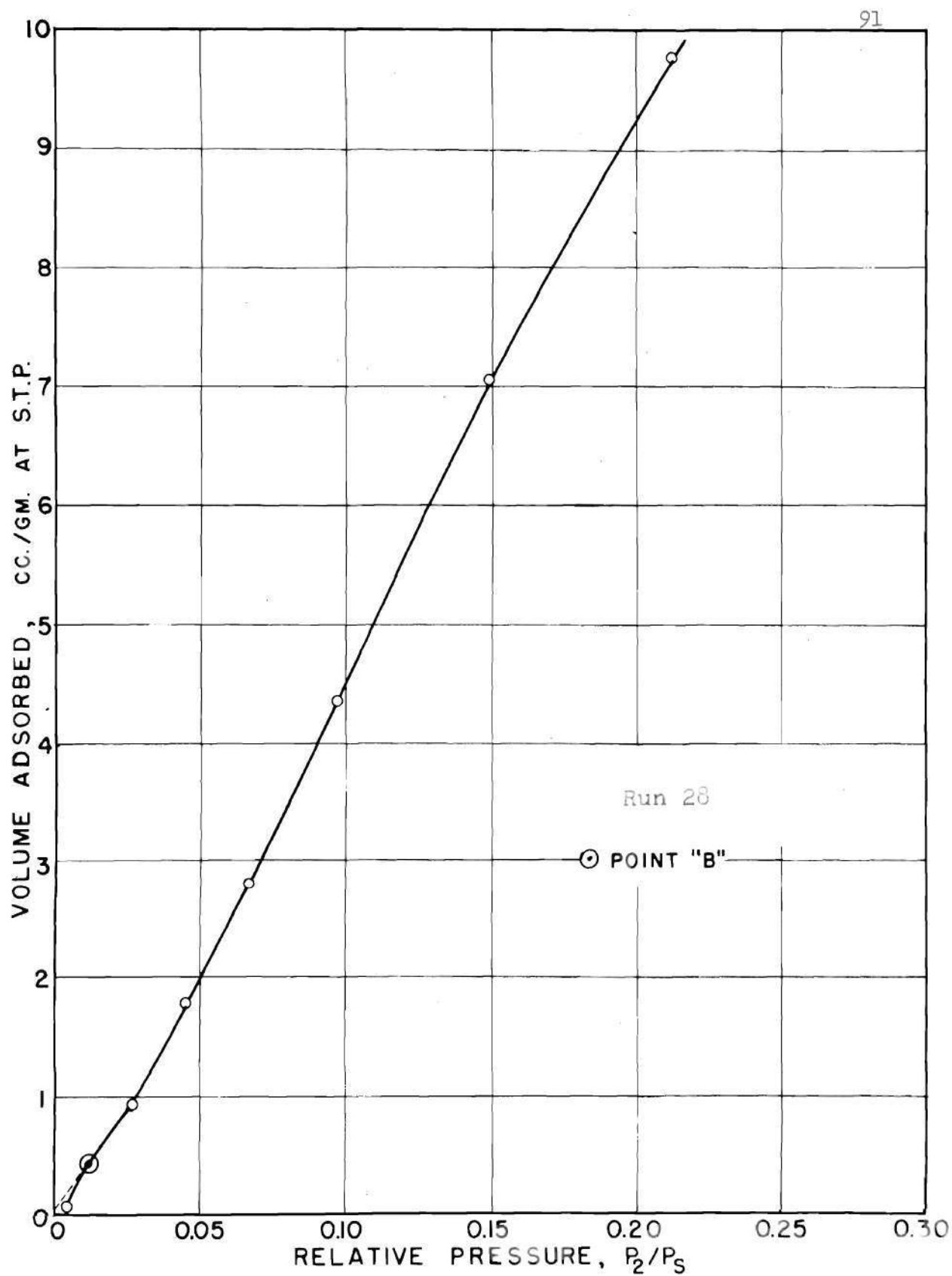


Figure 21. Adsorption of Nitrogen by No. 19 Glass Beads

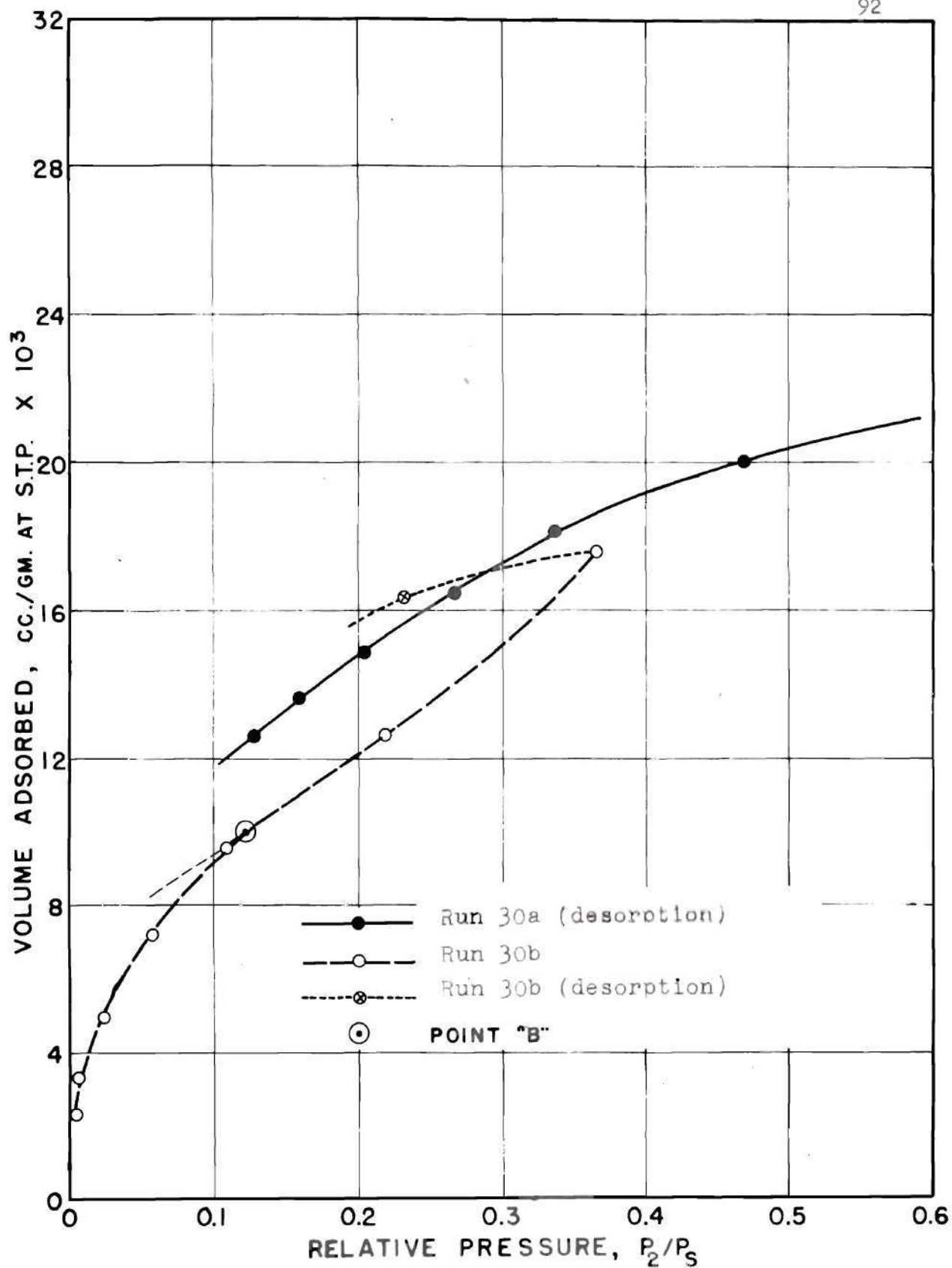


Figure 22. Adsorption of Ethane by No. 18 Glass Beads

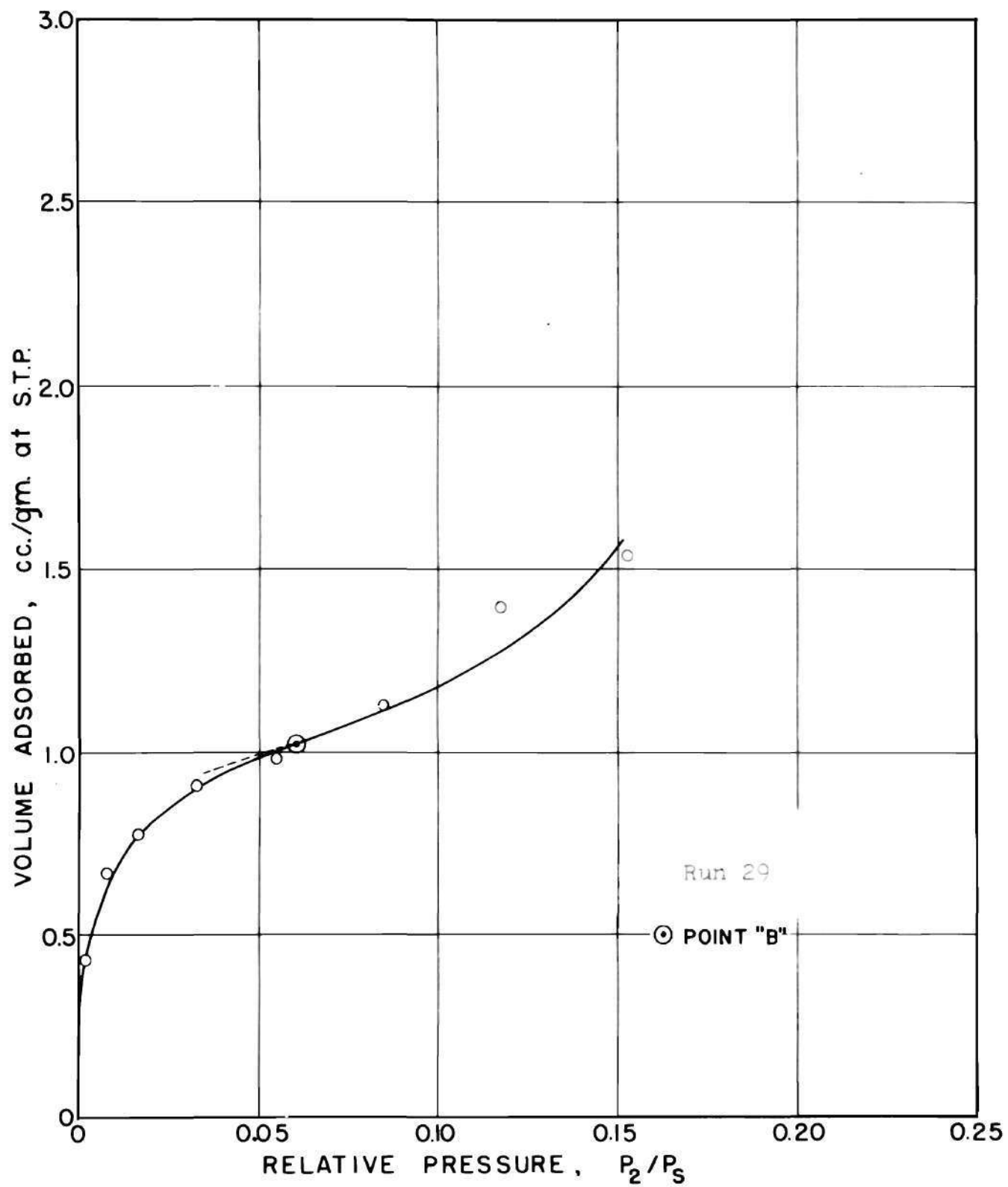


Figure 23. Adsorption of Nitrogen by Mica 432

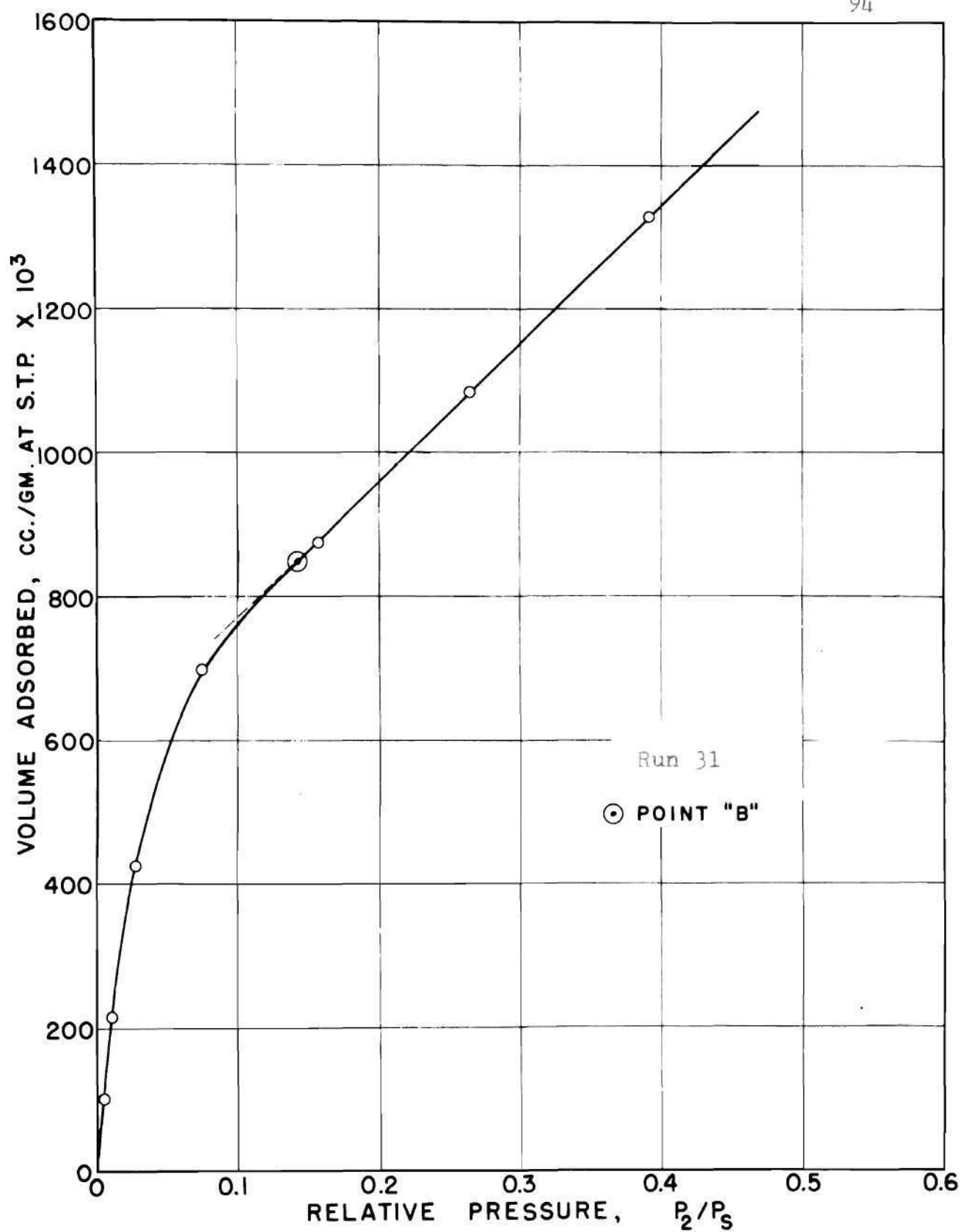


Figure 24. Adsorption of Ethane by Mica 432

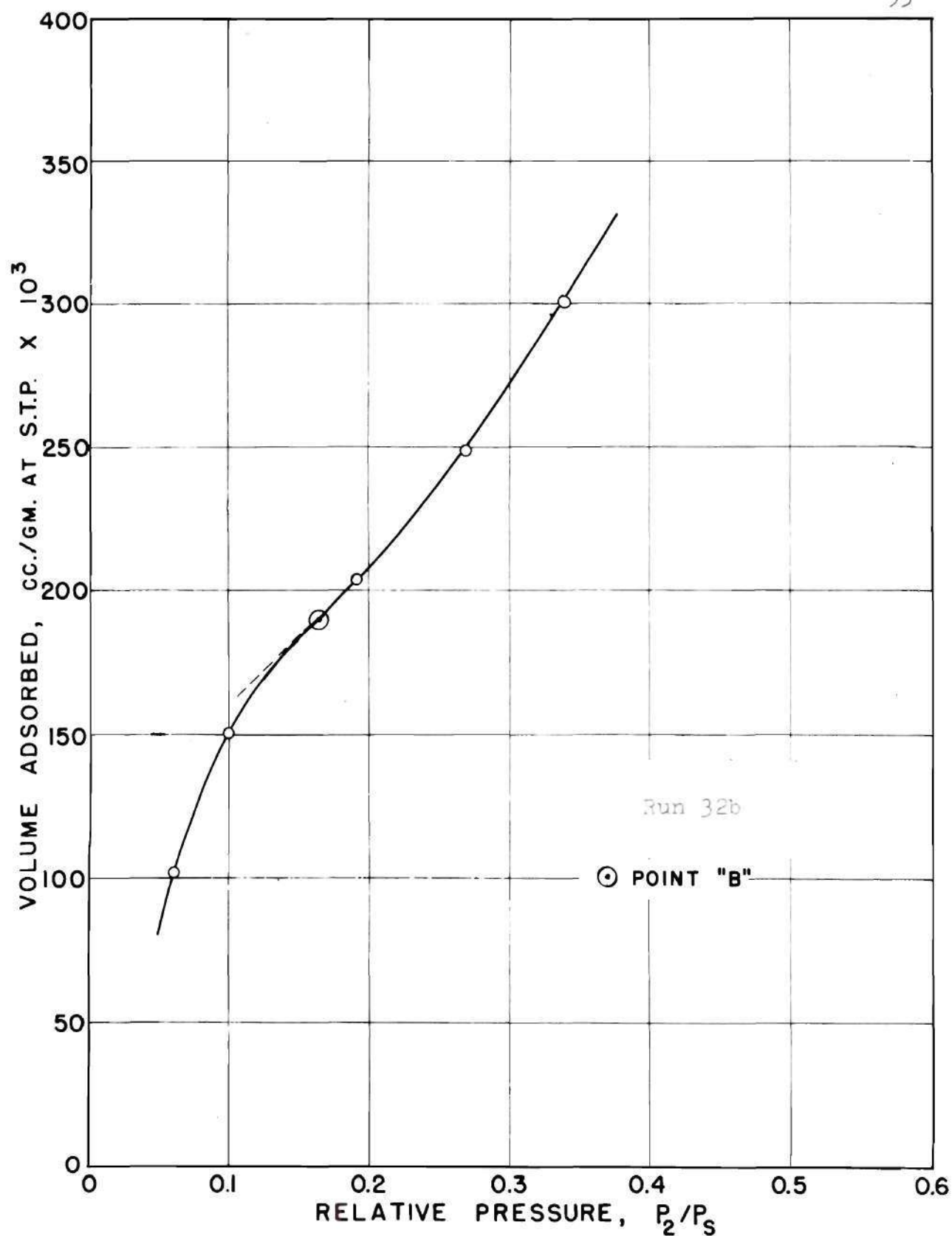


Figure 25. Adsorption of Ethane by Silica 196



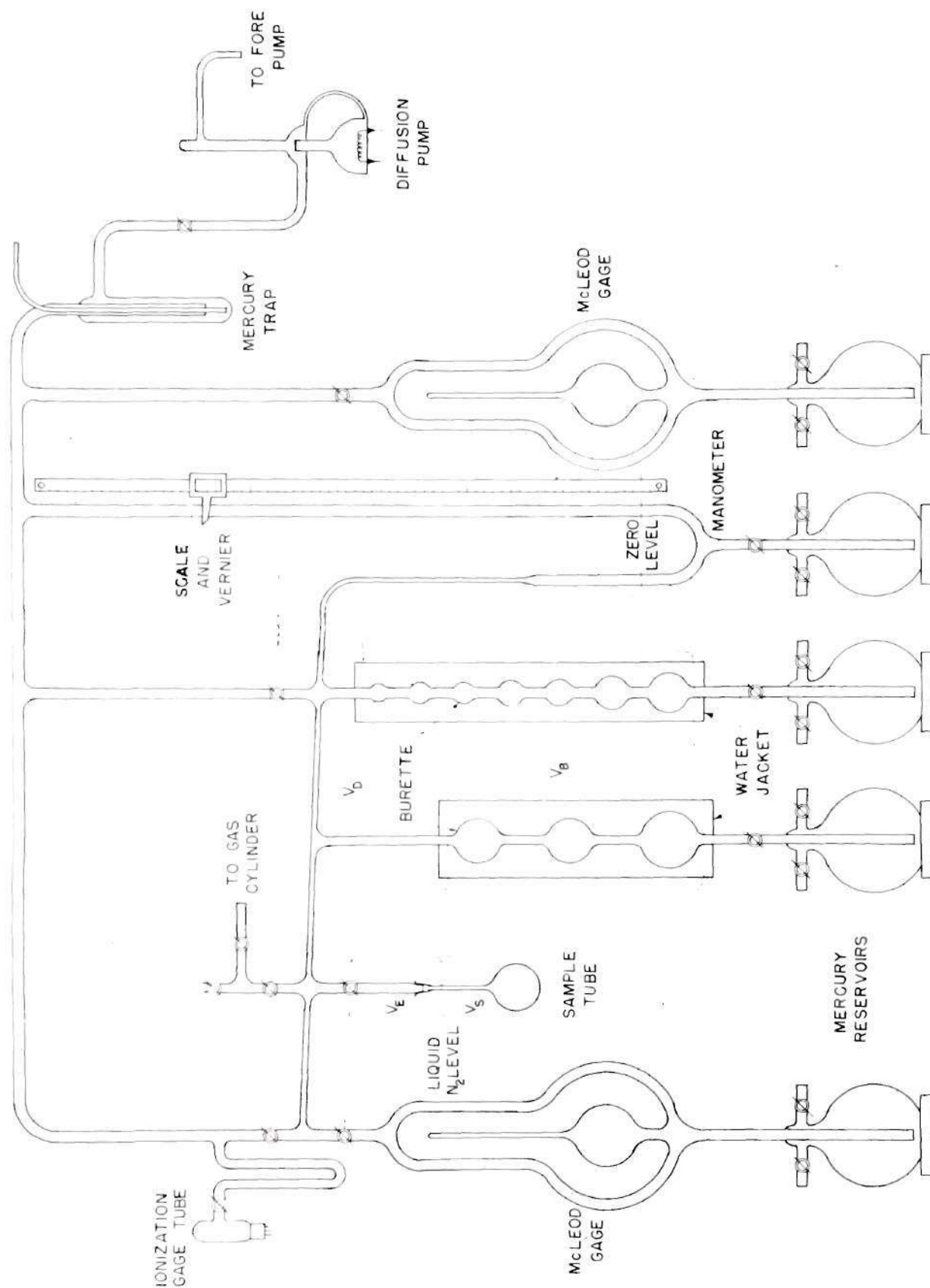


Figure 26. Schematic Diagram of NET Nitrogen Adsorption Apparatus

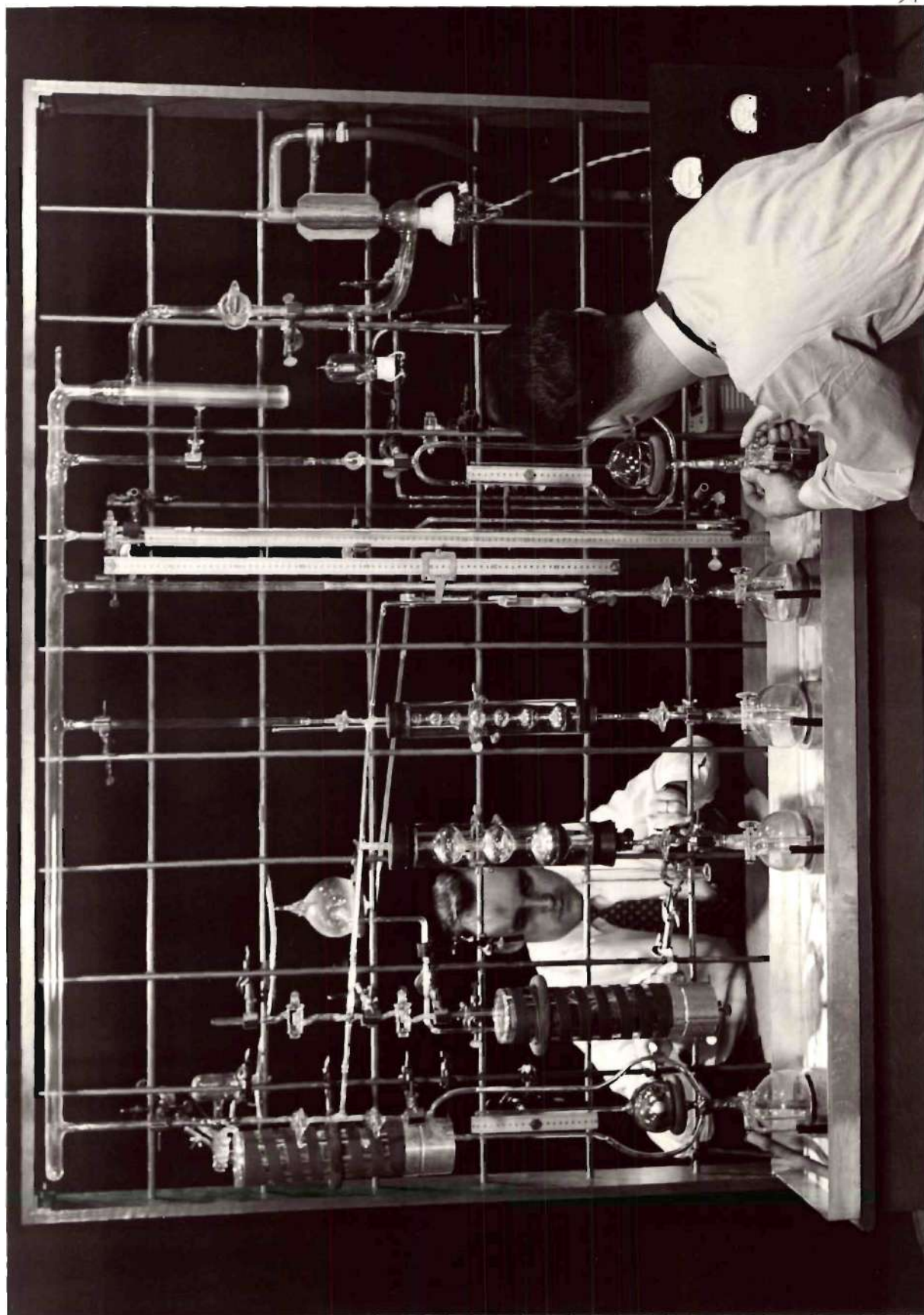


Figure 27. BET Nitrogen Adsorption Apparatus.

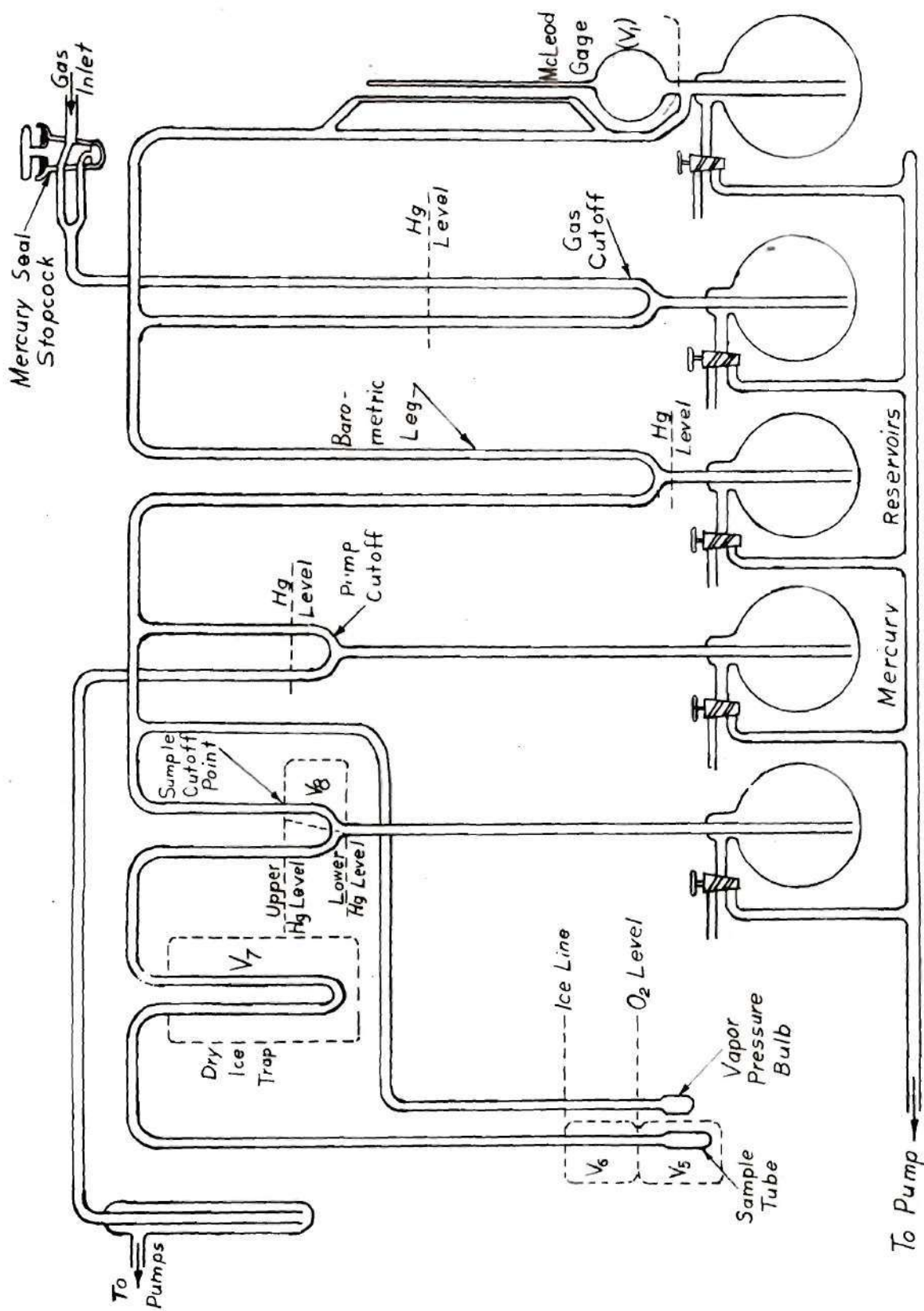


Figure 28. Schematic Diagram of BET(m) Ethane Adsorption Apparatus